
Investigating Compositional Reasoning in Time Series Foundation Models

Willa Potosnak¹ Cristian Challu^{*12} Mononito Goswami^{*1} Kin G. Olivares¹³ Michał Wiliński¹
Nina Żukowska¹ Artur Dubrawski¹

Abstract

Large pre-trained time series foundation models (TSFMs) have demonstrated promising zero-shot performance across a wide range of domains. However, a question remains: Do TSFMs succeed solely by memorizing training patterns, or do they possess the ability to reason? While reasoning is a topic of great interest in the study of Large Language Models (LLMs), it is undefined and largely unexplored in the context of TSFMs. In this work, inspired by language modeling literature, we formally define compositional reasoning in forecasting and distinguish it from in-distribution generalization. We evaluate the reasoning and generalization capabilities of 23 popular deep learning forecasting models on multiple synthetic and real-world datasets. Additionally, through controlled studies, we systematically examine which design choices in TSFMs contribute to improved reasoning abilities. Our study yields key insights into the impact of TSFM architecture design on compositional reasoning and generalization. We find that patch-based Transformers have the best reasoning performance, closely followed by residualized MLP-based architectures, which are 97% less computationally complex in terms of FLOPs and 86% smaller in terms of the number of trainable parameters. Interestingly, in some zero-shot out-of-distribution scenarios, these models can outperform moving average and exponential smoothing statistical baselines trained on in-distribution data. Only a few design choices, such as the tokenization method, had a significant (negative) impact on Transformer model performance.

1. Introduction

Foundation models have demonstrated an exceptional ability to generalize in zero-shot prediction tasks. Inspired by the success of such models in Natural Language Processing, recent work has adapted Transformers to build time series foundation models (TSFM). Zero-shot inference is particularly important for time series models, which must handle complex patterns, seasonal variations, and emerging trends where little to no reference data may be available.

To achieve zero-shot generalization, TSFMs are trained on increasingly large and diverse datasets, aiming to expand coverage and minimize unseen patterns. This raises a critical question: **Do TSFMs succeed by memorizing training patterns, or do they possess an ability to reason?** If TSFMs rely primarily on memorization, their ability to generalize to unseen data may be limited. In such cases, these memorization-dependent models would become overly reliant on training data and suffer from inefficient knowledge storage, requiring progressively larger models to generalize effectively. We argue that a good TSFM should be capable of *implicit reasoning*, enabling it to go beyond memorization and extrapolate unseen patterns. Such models would require fewer data points to generalize, utilize fewer parameters, and demonstrate greater robustness.

Although memorization and reasoning have been extensively studied in language models, their time series counterparts remain largely unexplored in these contexts and require investigation.

In this work, we take an initial step toward assessing the implicit reasoning abilities of neural forecasting models, with a focus on compositional reasoning—the ability to leverage and compose learned patterns from simpler forecasting tasks to generalize to more complex, unseen patterns. This definition refines out-of-distribution (OOD) generalization by emphasizing how learning fundamental patterns equips models to handle logically derived, more intricate scenarios.

The main contributions of this paper are:

- (i) **Reasoning Framework for Time Series.** We formally define compositional reasoning in time series and introduce a framework to evaluate neural models' reasoning capabilities in forecasting. Using spectral

^{*}Equal contribution ¹Auton Lab, School of Computer Science, Carnegie Mellon University ²Nixtla ³Amazon. Correspondence to: Willa Potosnak <wpotosna@andrew.cmu.edu>.

analysis, we assess various methods’ capacity to *logically* generalize to unseen periodic patterns through basis function extrapolation.

- (ii) **Large-Scale Study of Model Architectures and Design Components.** We evaluate the performance of 23 popular deep learning forecasting models on both synthetic and real-world datasets, identifying architectures that consistently demonstrate generalization and reasoning abilities. Additionally, through controlled studies, we systematically examine which design choices in TSFMs contribute to improved reasoning abilities.
- (iii) **Open-source Code and Data.** We introduce a synthetic dataset with arbitrarily complex time series, designed to evaluate compositional reasoning. The model, training framework, and datasets are open-source, enabling reproducible experimentation and supporting future studies on model reasoning. Our code is available at https://github.com/PotosnakW/neuralforecast/tree/tsfm_reasoning.

The rest of the paper is structured as follows. Section 2 reviews relevant literature. Section 3 introduces generalization and compositional-reasoning tasks. Section 4 contains our empirical findings. Finally, Section 5 discusses future research directions and concludes. Complementary material may be found in the Appendices.

2. Related Work

Reasoning in LLMs. Reasoning is a topic of great interest in the study of LLMs where prior work has developed experiments to elucidate various forms of reasoning (Allen-Zhu & Li, 2023; 2024; Wang et al., 2024; Yang et al., 2024b; Zhong et al., 2023). One of the most widely explored reasoning tasks is “composition”, which has also been referred to as “multi-hop” or chain-of-thought” reasoning. Compositional reasoning generally requires that a model combine multiple learned concepts observed during training to address a new question or prompt seen only during inference (Wang et al., 2024; Yang et al., 2024b; Zhong et al., 2023). For example, a composition task for an LLM might include training the model on specific sentences or facts represented as (subject, relation, object) triplets: “John’s friend is Jane” and “Jane is from NYC.” Given a new prompt at inference: “Where is John’s friend from?” the model is evaluated on whether it can generate the correct prediction of ‘NYC’, which requires that the model combine concepts from two facts seen due training. Mathematical reasoning via ‘addition’-like prompts has also been studied and similarly requires that a model can compose concepts observed during training. For example, given a new prompt, “Put together 5 and 40”, prior

work has shown that pre-trained LLMs implicitly compute addition with dimensions in the hidden state that represent numbers through sparse frequency-domain features (Zhou et al., 2024). Through curated experiments, such as this, language model reasoning is evaluated based on prediction matches, which can only be achieved if the model takes advantage of a specific reasoning strategy being tested. Similarly, for time series reasoning studies, it is crucial to design tailored experiments that effectively uncover reasoning capabilities—similar to those established in prior language model studies—with clear definitions of concepts, compositions, and evaluation strategies.

Reasoning in Time Series Foundation Models. Many foundation models have been proposed for time series forecasting (Wolff et al., 2024; Ansari et al., 2024b; Gao et al., 2024; Rasul et al., 2024; Woo et al., 2024; Goswami et al., 2024b; Das et al., 2024; Garza & Mergenthaler-Canseco, 2023; Liu et al., 2024d; Ekambaram et al., 2024). Recent work has primarily focused on extending the capabilities of these models using new architectures (Liu et al., 2024a; Shi et al., 2024) or by accounting for long and multivariate context (Żukowska et al., 2024; Liu et al., 2024c). Fewer studies have focused on what these models are learning and what contributes to their success. These studies have largely explored the concepts that TSFMs learn (Wiliński et al., 2024; Goswami et al., 2024b), the impact of scaling the model (Yao et al., 2024; Edwards et al., 2024), and their failure modes in controlled settings (Ansari et al., 2024a). However, to the best of our knowledge, no studies have explored whether the success of TSFMs stems from memorizing training data or from inherent reasoning abilities. Our study examines whether models can implicitly reason through the addition of concepts to facilitate effective zero-shot generalization to complex OOD time series.

3. Methods

3.1. Compositional Reasoning Forecasting Framework

In this section, we introduce our compositional reasoning forecasting framework and discuss its distinctions from the traditional forecasting paradigm.

Forecasting Task. Let a time series be denoted by $\mathbf{y}(t)$, with time $t \in \{1, \dots, T + H\}$. We consider a special regression problem that aims to learn a function $f : \mathcal{X} \mapsto \mathcal{Y}$, where the domain $\mathcal{X} = \{\mathbf{y}_{t-l:t}\}$ is composed of autoregressive context of length l , and codomain is the h -step future of a series $\mathcal{Y} = \{\mathbf{y}_{t+1:t+h}\}$. We denote the predictions:

$$\hat{\mathbf{y}}_{t:t+h} = f(\mathbf{y}_{t-l:t}). \tag{1}$$

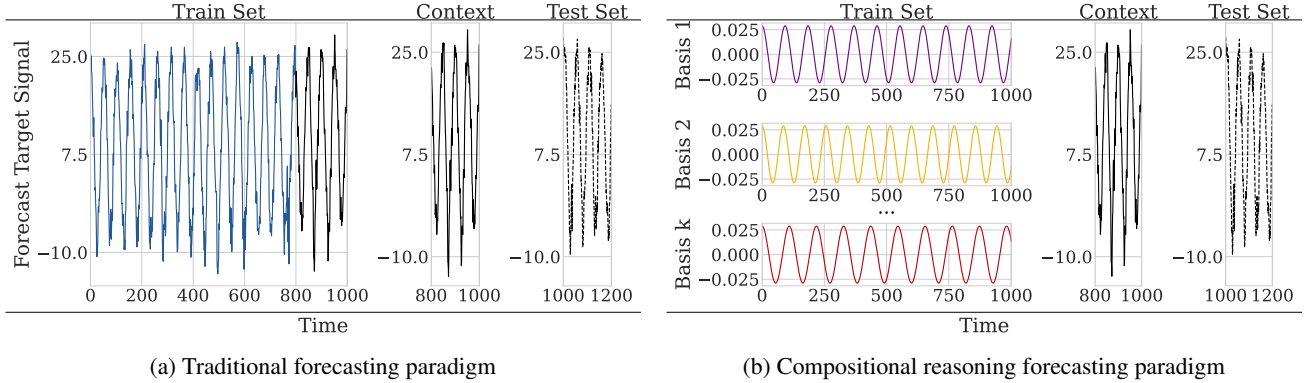


Figure 1. (a) Traditional forecasting paradigm: models are trained directly on the training set of forecast target signals, with forecasts for the temporally subsequent test set generated using the preceding context window. (b) Compositional reasoning forecasting paradigm: models are trained on basis function series that compose the ground truth signal, with forecasts for the temporally subsequent test set generated using the preceding context window.

Traditional Forecasting Paradigm. In the traditional forecasting paradigm, depicted in Fig. 1a, the train and test sets are defined by the non-overlapping sections of a time series, before and after a time T .

$$\mathcal{D}^{(train)} = \{(\mathbf{y}_{t-l:t}, \mathbf{y}_{t:t+h})\} \quad \text{with } t \leq T \quad (2)$$

$$\mathcal{D}^{(test)} = \{(\mathbf{y}_{t-l:t}, \mathbf{y}_{t:t+h})\} \quad \text{with } t > T \quad (3)$$

Under reasonable stationarity assumptions the train and test datasets will have a stable distribution, also known as an in-distribution (ID) forecast scenario

$$\mathbb{P}(\mathcal{D}^{(train)}) = \mathbb{P}(\mathcal{D}^{(test)}) \quad (4)$$

The traditional forecasting paradigm optimizes a parametrized model f_θ , which is used to generate forecasts for the test set. The model then is evaluated on the test set $\mathcal{D}^{(test)}$ using temporal cross-validation.

Compositional Reasoning Forecasting Paradigm. To test the compositional reasoning capabilities of forecasting models, as illustrated in Fig. 1b, we design a novel forecasting task where, instead of the original series $\mathbf{y}(t)$, the train dataset $\mathcal{D}^{(train)}$ consists of the top- k largest spectral components of $\mathbf{y}(t)$, obtained using Discrete Fourier Transform:

$$\text{If } \mathbf{y}(t) = \sum_{w=0}^T c_w e^{i \frac{2\pi w}{T} t}, \quad \text{then} \quad (5)$$

$$\mathcal{D}^{(train)} = \left\{ \left(e^{i \frac{2\pi w}{T} [t-l:t]}, e^{i \frac{2\pi w}{T} [t:t+h]} \right) \right\} \quad (6)$$

$$\text{with } t > T \quad \text{and } |c_w| \in \text{top-}k \left(\{|c_0|, |c_1|, \dots, |c_T|\} \right)$$

$$\mathcal{D}^{(test)} = \{(\mathbf{y}_{t-l:t}, \mathbf{y}_{t:t+h})\} \quad \text{with } t > T, \quad (7)$$

where c_w represents the Fourier coefficients associated with the frequency component w in the Fourier series expansion

of the time series $\mathbf{y}(t)$. As discussed in Section 2, compositional reasoning refers to a model’s ability to synthesize well-defined concepts to make accurate predictions. In our proposed compositional reasoning paradigm, we train models on the spectral decomposition of the time series and evaluate them on the original series. This approach allows us to assess a model’s ability to logically generalize to unseen periodic patterns through the synthesize of fundamental building blocks—specifically, sine and cosine basis functions.

By adopting this framework, we move beyond traditional ID generalization and instead create carefully crafted OOD scenarios, where the model can still succeed through its reasoning capabilities.

$$\mathbb{P}(\mathcal{D}^{(train)}) \neq \mathbb{P}(\mathcal{D}^{(test)}) \quad (8)$$

As models are evaluated in a zero-shot forecasting setting, generalization can be achieved only through the addition of time series basis functions seen during training, or *composition-type reasoning*.

3.2. Data

The datasets used in this study span both synthetic and real-world time series. Together, these datasets offer a broad spectrum of temporal frequencies, patterns, and domains for evaluating model compositional reasoning capabilities.

Synthetic Dataset. The synthetic dataset, characterized by controlled variations in frequency and amplitude, serves as a simplified benchmark for testing compositional capabilities of time series forecasting algorithms with ideal stationary and periodic series. We consider a set of sinusoidal functions, $\mathcal{F} = \{\mathcal{Y} : \mathcal{Y}(t) = a \sin(b2\pi t), a \cos(b2\pi t)\}$, where $a \in [1, 32]$ and $b \in [3, 32]$. For N time series each with m

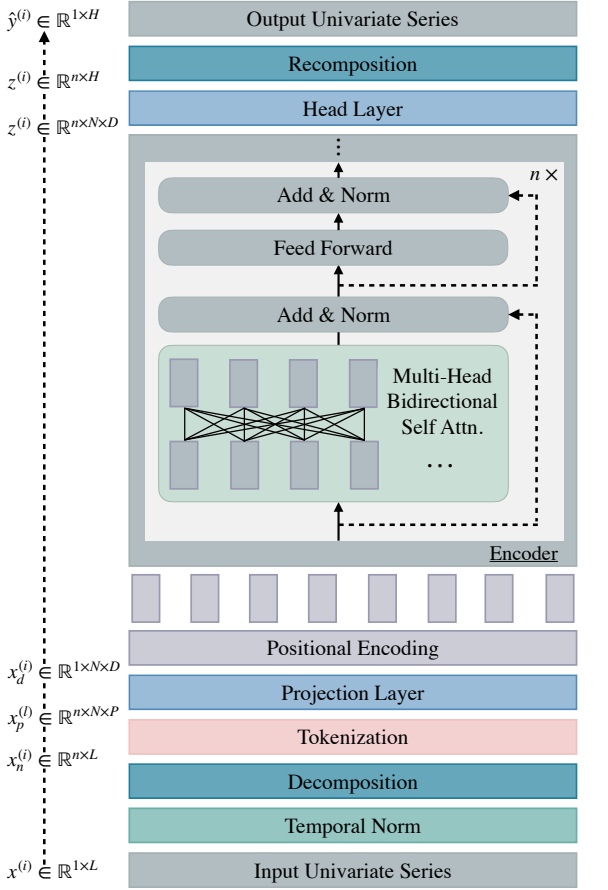


Figure 2. Transformer architecture based on the open-source T5 encoder backbone used in our controlled studies to evaluate various architecture components used across TSFMs. Architecture components for which no ablation studies are conducted are shown in gray.

signal compositions, the functions $\{\sin, \cos\}$ and parameters a and b are randomly sampled $m \times N$ times without replacement to generate the time series for each of the N compositional time series. The number of compositions is adjustable and serves as a parameter for experimentation. For our experiments, we generate $N = 100$ time series each comprised of only $m = 2$ signal compositions to first evaluate models on the simplest task possible with minimal compositions. More details about the dataset generation process are provided in Section A.5.

Real-World Datasets. We use widely studied time series datasets available in open-source repositories, including GIFT-Eval. (Aksu et al., 2024). The **Electricity Transformer Temperature (ETTm2)** dataset records measurements from an electricity transformer in a region of a province in China. It includes data on oil temperature and various load types, such as high useful load and high useless load, collected at 15-minute intervals between July 2016

and July 2018. The **Electricity (ECL)** dataset contains the hourly electricity consumption of 321 customers from 2012 to 2014. The **Solar** dataset contains hourly data on solar power generation in the US in 2006 (Aksu et al., 2024; Ansari et al., 2024a). The **Subseasonal** dataset contains climate time series data at the daily level (Mouatadid et al., 2023; Aksu et al., 2024). Modeling seasonal patterns at the daily resolution requires long context lengths, so we down-sample to weekly frequency to capture seasonal information within a manageable context length. The **Loop Seattle** dataset contains spatio-temporal speed data collected every 5 minutes from inductive loop detectors deployed on Seattle freeways (Cui et al., 2018; 2019). For our study, we use the downsampled 1-hour version of the dataset (Jiang et al., 2024; Aksu et al., 2024). More information on the datasets can be found in section A.6.

Preprocessing. We preprocess the real-world datasets by segmenting them into patches of 1056 time steps with a stride of 528, ensuring a consistent training set size of 1008. The forecast horizon is 48, consistent with the short-term prediction benchmarks in GIFT-Eval, such as ETTm2, Solar, and Loop Seattle (Aksu et al., 2024). We focus on stationary periodic subseries aligned with the synthetic dataset, as this alignment enables controlled experiments while avoiding the additional complexities of nonstationarity, which we leave for future work. To evaluate the stationarity of each series segment, we apply the Augmented Dickey-Fuller test ($\alpha = 0.001$) to identify and exclude series with extreme nonstationary characteristics from the final subset. From the refined set of stationary segments, we select the top 100 with the highest mean autocorrelation function (ACF) values for inclusion in the final dataset, ensuring consistency in the number of series across datasets.

3.3. Models

Baselines. We utilized ARIMA (Hyndman & Khandakar, 2008; Hyndman et al., 2024) and AutoETS (Brown, 1956) as our statistical baseline models.

Deep Learning Models. We trained models using 16 algorithms that cover a range of architectures and are widely used in practice. Trained models include: **Linear models:** DLinear (Zeng et al., 2023), NLinear (Zeng et al., 2023); **Multi-Layer Perceptron-based:** (MLP) (Rosenblatt, 1958), NHITS (Challu et al., 2022), NBEATS (Oreshkin et al., 2020; Olivares et al., 2022a), and TSMixer (Chen et al., 2023); **Recurrent Neural Network-based:** Long-Short Term Memory (LSTM) (Sak et al., 2014); **Convolutional Neural Network-Based:** Temporal Convolution Network (TCN) (Bai et al., 2018; van den Oord et al., 2016) and TimesNet (Wu et al., 2023); and **Transformer-Based:** VanillaTransformer (Vaswani

et al., 2017; Zhou et al., 2021), inverted Transformer (iTransformer) (Liu et al., 2024b), Autoformer (Wu et al., 2021), Informer (Zhou et al., 2021), Temporal Fusion Transformer (TFT) (Lim et al., 2021), and patch time series Transformer (PatchTST) (Nie et al., 2023). More information on these models, as well as model training and hyperparameters, is provided in Appendix A.2 and A.7.

T5-based Time Series Foundation Models. In addition to the aforementioned models, we aim to evaluate reasoning abilities of TSFMs. TSFMs are combinations of many architectural component design decisions, as summarized in Table 2. Comparing the performance of open-source TSFM models on compositional reasoning tasks alone does not allow us to isolate performance improvements attributable to specific components. To address this, we implement a deep learning Transformer architecture using the open-source T5 Model backbone, designed with modular components to enable flexible experimentation with various design decisions commonly employed in TSFMs, allowing for controlled testing. We pick T5 as the Transformer backbone as these are an open source family of LLMs of varying sizes, with efficient implementations, both encoders and decoders, and used by existing TSFMs (Żukowska et al., 2024; Goswami et al., 2024b). The basic Transformer architecture, illustrated in Fig. 2, incorporates diverse design choices, including input series tokenization (e.g., patching, binning), model size (e.g., tiny, mini), projection layer types (e.g., linear layers, residual networks), scalars (e.g., standard, robust), loss functions (e.g., mean squared error, quantile loss), attention mechanisms (e.g., bidirectional, causal), and positional encodings (e.g., sincos, relative). Additionally, we conduct ablation studies on context length, token (patch) length, and input series decomposition, the latter being inspired by models such as DLinear and Autoformer. An outline of the various component types and parameters for each design decision ablation is included in Table 3. This controlled setup is crucial for directly comparing architectures under identical conditions. By evaluating Transformer models with key components aligned with various TSFM design choices, our work provides valuable insights into which TSFM design decisions are better suited for reasoning in OOD scenarios.

3.4. Evaluation

We evaluated model forecasts by computing the MAE across all dataset series,

$$\text{MAE}(\mathbf{y}_\tau, \hat{\mathbf{y}}_\tau) = \frac{1}{H} \sum_{\tau=t+1}^{t+H} |\mathbf{y}_\tau - \hat{\mathbf{y}}_\tau|, \quad (9)$$

and report the average and standard deviation of the results for three random seeds. To assess compositional reasoning performance, we compute the error of the top $k = \{1, 2, \dots, 100\}$ Fourier basis function compositions

and calculate the average number of top k compositions each model can outperform over the datasets.

To compare different models, we use statistical tests used by prior work (Ismail Fawaz et al., 2019; Goswami et al., 2024a). For comparisons of three or more models, the Friedman test ($\alpha = 0.2$) is used to determine whether significant performance differences exist, testing the null hypothesis that all methods perform equally on average. If the null hypothesis is rejected, a post-hoc analysis is conducted using the Wilcoxon signed-rank test with Holm correction. The Wilcoxon test highlights specific pairs of models with statistically significant performance differences, while the Holm correction controls for Type I errors across multiple hypothesis tests. Critical difference (CD) diagrams proposed by Demšar (2006) were used visualize model average rank over the datasets based on forecasting error, or average MAE computed over three random seeds for each dataset. In addition to showing model rank, CD diagrams were used to highlight whether the performance of two models is significantly different based on the Wilcoxon signed-rank test with Holm correction. A thick horizontal line groups a set of models that are not significantly different.

4. Results

Patch-based Transformers & MLP-based models show sparks of compositional reasoning. Transformer-based models that ‘patch’ input time series, including PatchTST and the T5 Model, as well as MLP-based models, such as MLP, NHITS, and NBEATS, achieve the highest number of wins as one of the top three models for compositional reasoning tasks on OOD data, as shown in Table 1 and Fig. 4a. Standard deviation results for all models in Table 1 are provided in Table 6 in Appendix B.4. Moreover, these models as well as TimesNet and TFT were the only models to outperform at least 2 basis function compositions on average across the datasets, indicating some implicit reasoning capacity through composition of basis signals. The top k basis wins for ID and OOD data are shown in Table 1 and in Fig. 5. Among these, the T5 Model and NBEATS achieve the highest number of wins as one of the top three models as well as the highest number of average top k basis function composition wins for OOD data. The composition win average for these two models achieved at least 18% of their wins for ID data. Example forecasts for these models on the Subseasonal dataset shown in Fig. 3 highlights generalization achieved through compositional reasoning. Forecast examples for all 6 datasets are provided in Figs. 9 and 10 in Appendix B.2.

Zero-shot T5 in OOD scenarios can improve upon statistical model baselines trained on ID data. Zero-shot forecasts for the T5 Model, NHITS, NBEATS, and MLP models in OOD scenarios via the compositional reasoning fore-

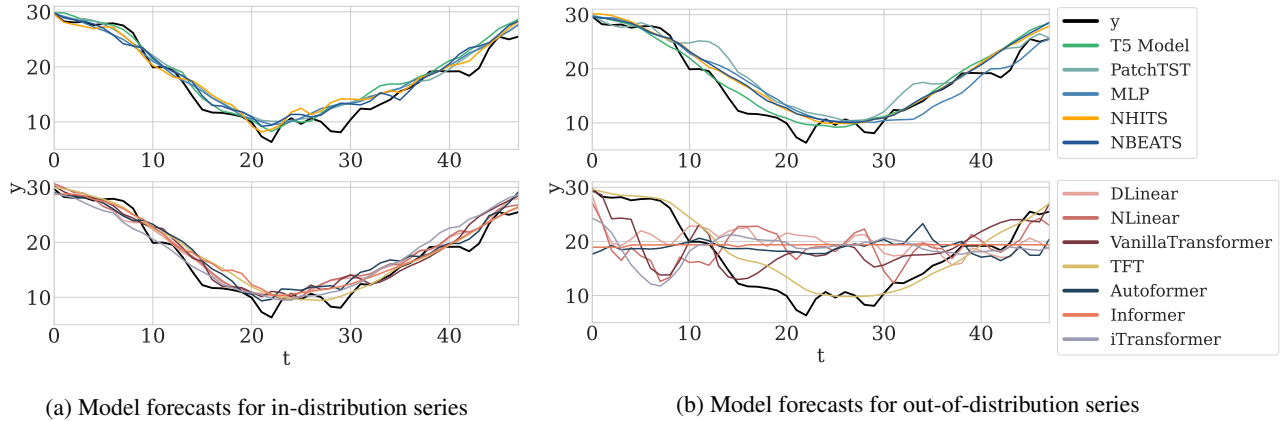


Figure 3. (a) Forecasts for a ground truth series $y(t)$ for the Subseasonal dataset for models trained using the traditional forecasting paradigm. (b) Forecasts for models trained using the compositional reasoning forecasting paradigm. Patch-based Transformer models and MLP-based models (top) demonstrate effective generalization to out-of-distribution time series, whereas other Transformer variants and linear models struggle to do so (bottom).

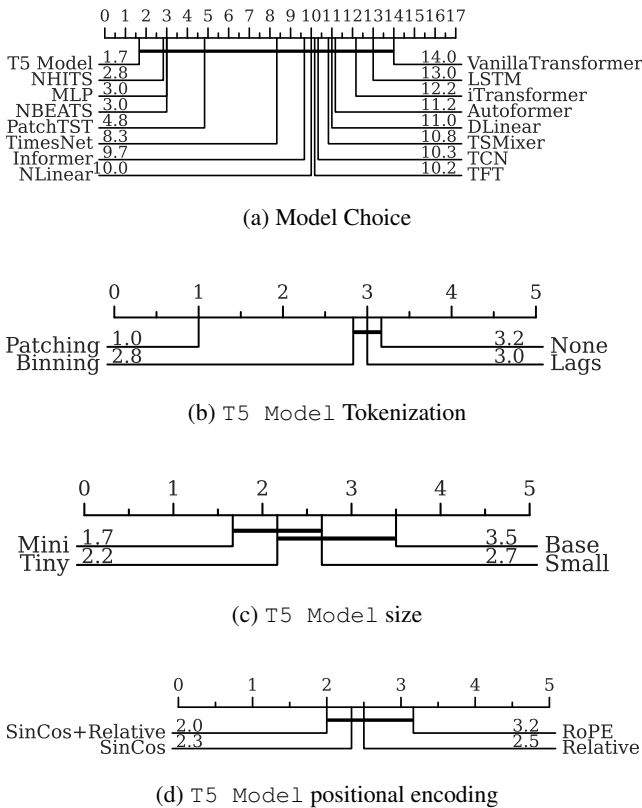


Figure 4. Critical difference diagrams showing performance ranks for composition reasoning tasks across datasets for various (a) models and (b, c, e) T5 Model model design decisions. Lower ranks indicate better performance. A thick horizontal line groups a set of models that are not significantly different using the Wilcoxon signed-rank test with Holm correction.

casting paradigm can outperform moving average forecasts for ARIMA models trained on ID data across all 6 datasets. These same models can also outperform `AutoETS` model forecasts for 2 of 6 datasets. All other models can outperform both statistical baselines for 1 of 6 datasets. This result underscores the effectiveness of T5 Model and residualized MLP-based architectures in zero-shot forecasting for stationary OOD data. It also suggests that such models trained on various concepts, or basis functions, may serve as strong baseline candidates alongside statistical models for effective generalization in OOD scenarios.

Better “reasoners” can also be computational efficient.

The T5 Model, MLP, NHITS, and NBEATS models demonstrate lower computational complexity in terms of floating-point operations per second (FLOPs) compared to many other Transformer, RNN, and CNN models. However, the T5 Model model exhibits the second largest size in terms of total trainable parameters, whereas models such as MLP, NHITS and NBEATS have much smaller footprints, as shown in Fig. 6. Performance versus FLOPs plots for both ID and OOD scenarios are provided in Appendix B.3.

Input patching enables Transformer-based TSFMs, while other tokenization methods degrade performance.

We observe that the T5 Model with fixed-length patches significantly outperforms different tokenization methods in compositional reasoning tasks, as shown in Fig. 8b. Patch-based tokenization also ranks highest for experiments on ID series. For other T5 Model model ablations, we observe that model size and projection layer also demonstrate statistically significant differences across methods as shown in Figs. 8d, 8b, 8h, respectively. Other design decisions, such as attention type, token length, positional encoding, loss functions, input/output scaling functions, context length,

Table 1. Mean Absolute Error (MAE) averaged over 3 random seeds for model forecasts. The out-of-distribution (OOD) column presents MAE results for models trained via the compositional reasoning forecasting paradigm. The in-distribution (ID) column presents MAE results for models trained via the traditional forecasting paradigm. PatchTST and the T5 Model with the best patch length (PL) from Tables 6 and 7 are included. Best results are highlighted in **bold**, second best results are underlined. The count of instances across datasets where the model ranks in the top three for performance is shown in the second to last column with non-zero entries in **blue**. The average number of top k compositions the model can outperform over the datasets is shown in the last column with nonzero entries in **purple**.

Model	Synthetic Sinusoid		ECL		ETM2		Solar		Subseasonal		Loop Seattle		Top 3 Win Count		Top k Basis Wins	
	OOD	ID	OOD	ID	OOD	ID	OOD	ID	OOD	ID	OOD	ID	OOD	ID	OOD	ID
ARIMA	-	15.538	-	0.822	-	0.332	-	9.687	-	7.855	-	8.638	-	0	-	0.5
AutoETS	-	16.075	-	0.105	-	0.211	-	1.730	-	2.067	-	5.575	-	0	-	0.8
DLinear	12.991	12.460	0.820	<u>0.103</u>	0.330	0.135	9.925	1.555	8.042	1.496	9.085	4.293	0	2	0.2	55.5
NLinear	13.287	13.056	0.801	0.104	0.325	0.136	9.681	<u>1.569</u>	8.436	1.509	9.026	4.307	0	1	0.3	53.7
MLP	<u>8.647</u>	2.475	<u>0.283</u>	0.106	0.253	0.114	<u>4.826</u>	1.559	1.886	1.456	7.839	3.864	3	1	10.2	61.2
NHITS	8.924	1.106	0.295	0.101	0.214	0.100	5.682	1.592	1.858	<u>1.135</u>	<u>7.747</u>	3.448	4	4	11.0	64.3
NBEATS	8.907	1.383	0.294	<u>0.103</u>	<u>0.216</u>	<u>0.102</u>	5.852	1.599	<u>1.840</u>	1.177	7.763	3.479	5	4	11.2	61.8
TSMixer	14.466	15.090	0.799	0.129	0.335	0.182	9.877	1.979	7.770	1.602	8.865	5.565	0	0	0.3	19.7
LSTM	13.410	4.238	0.835	0.110	0.337	0.135	10.241	1.717	8.095	1.545	9.465	3.703	0	0	0	48.7
TCN	11.478	3.833	0.837	0.106	0.339	0.135	9.868	1.642	6.170	1.234	8.792	<u>3.422</u>	0	1	0.7	55.7
TimesNet	9.788	<u>2.451</u>	0.518	0.104	0.313	0.109	9.914	1.714	4.109	1.500	9.872	2.970	0	2	2.3	52.8
VanillaTransformer	12.279	4.935	0.919	0.106	0.334	0.136	11.956	1.667	9.641	1.276	11.675	3.591	0	0	0.2	54.8
iTransformer	15.478	15.203	0.829	0.157	0.326	0.196	9.822	1.805	8.447	1.628	9.182	4.871	0	0	0.2	23.5
Autoformer	15.301	15.018	0.795	0.137	0.330	0.294	10.348	2.108	7.933	2.390	8.634	4.758	0	0	0.3	15.8
Informer	14.353	10.144	0.787	0.128	0.321	0.141	8.351	1.662	6.878	1.564	11.549	4.241	0	0	0.5	41.0
TFT	14.531	9.745	0.445	0.115	0.312	0.117	12.873	2.106	2.684	1.454	11.280	5.340	0	0	4.7	28.5
PatchTST (Best PL)	10.696	6.959	0.482	0.122	0.247	0.138	5.726	1.633	2.185	1.659	7.965	3.653	1	0	7.8	45.2
T5 Model (Best PL)	7.177	2.480	0.239	<u>0.103</u>	0.259	0.103	3.899	1.578	1.714	1.097	6.589	3.351	5	4	12.2	64.3

input decomposition did not demonstrate statistically significant differences as shown in Fig. 8 in Appendix B.1.

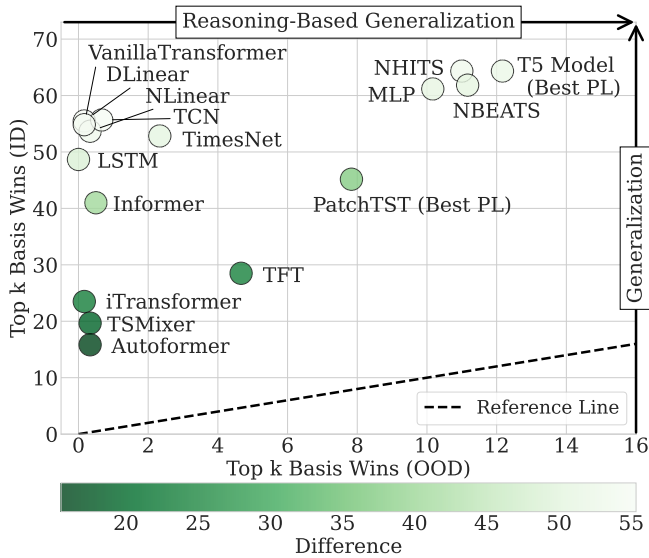


Figure 5. The average number of top k compositions that models can outperform across datasets for ID and OOD data. The difference in wins between ID and OOD data is shown in green, with lighter colors indicating larger deviations. As the average number of top k compositions outperformed increases for OOD data, models demonstrate better generalization through compositional reasoning. Patch-based Transformers and MLP-based models outperform others in reason-based generalization for OOD scenarios. Models in the top right corner perform well on ID tasks but show less evidence of compositional reasoning capabilities.

Architecture choices that perform well for ID series do not necessarily perform well for OOD series. Some models demonstrate consistently higher performance across both ID and OOD data, such as models like NHITS, NBEATS, MLP and the T5 Model. However, our ablation studies with the T5 Model reveal that certain architecture components choices that that perform well for ID series do not necessarily perform well for OOD series. In particular, smaller models rank higher in performance than larger models in compositional reasoning tasks across datasets, whereas larger models outperform smaller models in the general train/test paradigm, as shown in Figs. 8c and 8d. Similarly, while using residual networks for projection layers may improve performance for ID tasks it performs significantly worse for compositional reasoning tasks. CD diagrams for each architecture design component are included in Figs. 7 and 8 in Appendix B.1.

5. Discussion

Our experiments yield key insights into TSFM architecture design that enable both reasoning and generalization. We find that: (1) Transformer-based models adapted from LLMs, such as T5, rank among the best in generalization and compositional reasoning tasks; (2) input patching unlocks reasoning capabilities in Transformer-based TSFMs, whereas other input tokenization methods degrade T5 models performance; and (3) MLP-based architectures are a close second with an average MAE difference of 17% across datasets. NHITS is the second-best model, which is approximately 97% more computationally efficient in terms of

FLOPs and 86% smaller in terms of the number of trainable parameters. For models trained on ID data, the T5 Model and MLP-based models, such as NHITS, NBEATS, and MLP, rank among the best in generalization, followed by CNN-based models, TimesNet and TCN, respectively.

Our findings provide critical insights for the future development of scalable and reasoning-capable TSFMs. Based on our experiments, practitioners seeking to build more reasoning-capable TSFMs should explore input series tokenization strategies that preserve local information, such as ‘patching’. Hierarchical decomposition used by methods such as NBEATS and NHITS to simplify complex temporal patterns into structured concepts for additive modeling present a promising approach. However, extracting concepts like seasonality using moving average filters may be insufficient, as evidenced by the performance of DLinear, Autoformer, and the moving average decomposition ablation for T5 Model (Table 7). Instead, architectures with concept-specialized ‘stacked’ processing, such as NHITS and NBEATS, show greater potential for enhancing model compositional reasoning performance. Additionally, while the T5-efficient-base model ranks the highest in performance for ID forecasting tasks, increased model size does not translate to improved compositional reasoning performance as shown by the statistically significant difference between T5-efficient-mini and T5-efficient-base in Fig. 4c. Therefore, future research on TSFMs should prioritize innovating new architectural components over simply scaling model size.

In our study, we identified models that do not show evidence of compositional reasoning using a simple yet effective metric: their ability to outperform the composition of the top $k = 2$ basis functions, indicating minimal compositional capabilities. Our results show that only 7 of 16 models pass this test. This top k metric provides a simple threshold for evaluating the reasoning capabilities of models, and can be scaled to higher and more challenging basis function composition thresholds. By ruling out compositional reasoning for some models, our findings suggest that those models may rely on alternative forms of reasoning or memorization to generalize in traditional forecasting paradigms. This work takes an initial step in exploring reasoning in TSFMs. By providing open-source code, we aim to facilitate future research, ultimately advancing our understanding of reasoning versus memorization in time series forecasting models.

Limitations. This study has two limitations in relation to data. First, we focus on stationary time series as an initial step in evaluating compositional reasoning capabilities. Future work should extend the provided compositional reasoning framework for assessments with non-stationary time series. For instance, evaluating model compositional reasoning capabilities for concepts such as trend in addition to

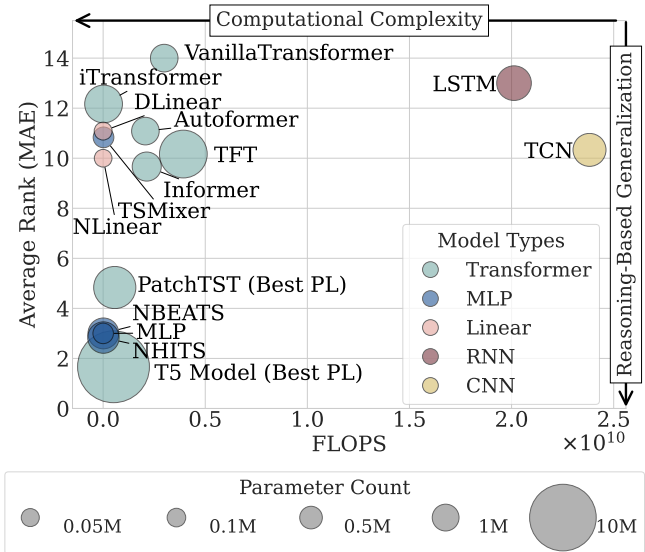


Figure 6. Comparison of average rank across datasets and random seeds versus model efficiency, measured in FLOPs. The size of each point represents the number of trainable parameters. Models in the lower left corner demonstrate better generalization in compositional reasoning tasks and lower computational complexity.

the stationary basis functions used in this study. The second limitation is that, due to the computational cost and time required for training, we evaluated the compositional capabilities of the model using five open-source datasets. Although these data sets provide valuable information, incorporating more data sets may help to elucidate other significant performance differences between model architecture component methods. To address this limitation, we provide open source code for our compositional reasoning framework, allowing the community to incorporate additional datasets and conduct further experiments with minimal effort.

Future Work. We focus ablation experiments on the best-performing architecture, the T5 Model. Future work can expand ablations to other promising architectures, such as NBEATS and NHITS, and explore additional novel TSFM architecture components. Future work can also explore alternative hyperparameter configurations and convergence-based stopping criteria for model training, beyond early stopping with a fixed number of validation iterations.

Reasoning in TSFMs, similar to LLMs, can take various forms, with this work focusing primarily on compositional reasoning. Other reasoning types, such as ‘comparison’ and ‘inverse search,’ which have been explored in LLMs, may also play an important role in TSFM performance. Future research should investigate these alternative reasoning forms in time series models to better understand their impact on generalization across diverse datasets. The open-source code provided in this study can serve as a foundation for

extending research on model reasoning and generalization by incorporating additional or novel TSFM architecture component methods.

Acknowledgements

This work was partially supported by the NSF (awards 2406231 and 2427948), NIH (awards R01NS124642 and R01DK131586), DARPA (HR00112420329), and the US Army (W911NF-20-D0002).

Impact Statement

This study investigates whether time series models can perform implicit reasoning during zero-shot inference by synthesizing learned concepts to generalize to more complex data patterns. Our findings reveal that certain models can generalize effectively in well-designed OOD scenarios, highlighting reasoning abilities that go beyond basic pattern memorization. As this work is exploratory and not tied to specific applications, we do not foresee any negative societal impacts. In contrast, our insights could aid in the development of more data- and computationally-efficient deep learning architectures. Additionally, our results can help identify the limitations of time series models, ensuring that they are not used in scenarios where poor generalization is likely.

Reproducibility Statement

The models were implemented using the `Neuralforecast` library (Olivares et al., 2022b). The open-source code for generating critical difference diagrams is available at <https://github.com/hfawaz/cd-diagram>. All datasets used in this study are publicly accessible and can be downloaded by following the instructions at <https://github.com/SalesforceAIResearch/gift-eval>. Model training and evaluation were conducted on a computing cluster equipped with 128 AMD EPYC 7502 CPUs, 503 GB of RAM, and 8 NVIDIA RTX A6000 GPUs, each with 49 GiB of RAM. To ensure reproducibility, the model implementations, training framework, and datasets are open-source, supporting future research on model reasoning. The complete codebase is available at https://github.com/PotosnakW/neuralforecast/tree/tsfm_reasoning.

References

Aksu, T., Woo, G., Liu, J., Liu, X., Liu, C., Savarese, S., Xiong, C., and Sahoo, D. Gift-eval: A benchmark for general time series forecasting model evaluation, 2024. URL <https://arxiv.org/abs/2410.10393>.

Allen-Zhu, Z. and Li, Y. Physics of language models: Part 3.2, knowledge manipulation, 2023.

Allen-Zhu, Z. and Li, Y. Physics of language models: Part 3.1, knowledge storage and extraction. In *Proceedings of the 41st International Conference on Machine Learning*, pp. 235, 2024.

Ansari, A. F., Stella, L., Turkmen, C., Zhang, X., Mercado, P., Shen, H., Shchur, O., Rangapuram, S. S., Arango, S. P., Kapoor, S., Zschiegner, J., Maddix, D. C., Mahoney, M. W., Torkkola, K., Wilson, A. G., Bohlke-Schneider, M., and Wang, Y. Chronos: Learning the language of time series, 2024a.

Ansari, A. F., Stella, L., Turkmen, C., Zhang, X., Mercado, P., Shen, H., Shchur, O., Rangapuram, S. S., Arango, S. P., Kapoor, S., Zschiegner, J., Maddix, D. C., Wang, H., Mahoney, M. W., Torkkola, K., Wilson, A. G., Bohlke-Schneider, M., and Wang, Y. Chronos: Learning the language of time series. *Transactions on Machine Learning Research*, 2024b.

Bai, S., Kolter, J. Z., and Koltun, V. An empirical evaluation of generic convolutional and recurrent networks for sequence modeling, 2018.

Brown, R. G. Exponential smoothing for predicting demand. *Philip Morris Records*, 1956.

Cai, Y., Choudhry, A., Goswami, M., and Dubrawski, A. Timeseriesexam: A time series understanding exam. *NeurIPS 2024 Workshop on Time Series in the Age of Large Model*, 2024.

Challu, C., Olivares, K. G., Oreshkin, B. N., Garza, F., Mergenthaler-Canseco, M., and Dubrawski, A. N-HiTS: Neural hierarchical interpolation for time series forecasting. In *AAAI-23*, 2022.

Chen, S.-A., Li, C.-L., Yoder, N. C., Ö. Arık, S., and Pfister, T. TSMixer: An all-MLP architecture for time series forecasting. In *Published in Transactions on Machine Learning Research*, 2023.

Chow, W., Gardiner, L., Hallgrímsson, H. T., Xu, M. A., and Ren, S. Y. Towards time-series reasoning with llms. *NeurIPS 2024 Workshop on Time Series in the Age of Large Model*, 2024.

Cui, Z., Ke, R., and Wang, Y. Deep bidirectional and unidirectional lstm recurrent neural network for network-wide traffic speed prediction. *arXiv preprint arXiv:1801.02143*, 2018.

Cui, Z., Henrickson, K., Ke, R., and Wang, Y. Traffic graph convolutional recurrent neural network: A deep learning

- framework for network-scale traffic learning and forecasting. *IEEE Transactions on Intelligent Transportation Systems*, 2019.
- Das, A., Kong, W., Sen, R., and Zhou, Y. A decoder-only foundation model for time-series forecasting, 2024.
- Demšar, J. Statistical comparisons of classifiers over multiple data sets. In *Journal of Machine Learning Research*, pp. 1–30, 2006.
- Edwards, T. D., Alvey, J., Alsing, J., Nguyen, N. H., and Wandelt, B. D. Scaling-laws for large time-series models. *arXiv preprint arXiv:2405.13867*, 2024.
- Ekambaram, V., Jati, A., Nguyen, N. H., Dayama, P., Reddy, C., Gifford, W. M., and Kalagnanam, J. TTMs: Fast Multi-level Tiny Time Mixers for Improved Zero-shot and Few-shot Forecasting of Multivariate Time Series. *arXiv preprint arXiv:2401.03955*, 2024.
- Fukushima, K. Cognitron: A self-organizing multilayered neural network. *Biol. Cybernetics*, 20:121–136, 1975.
- Gao, S., Koker, T., Queen, O., Hartvigsen, T., Tsiligkaridis, T., and Zitnik, M. Units: A unified multi-task time series model. In *The Thirty-eighth Annual Conference on Neural Information Processing Systems*, 2024.
- Garza, A. and Mergenthaler-Canseco, M. TimeGPT-1, 2023.
- Goswami, M., Sanil, V., Choudhry, A., Srinivasan, A., Udompanyawit, C., and Dubrawski, A. Aqua: A benchmarking tool for label quality assessment. *Advances in Neural Information Processing Systems*, 36, 2024a.
- Goswami, M., Szafer, K., Choudhry, A., Cai, Y., Li, S., and Dubrawski, A. MOMENT: A family of open time-series foundation models. In *41st International Conference on Machine Learning*, 2024b.
- Hanna, M., Liu, O., and Variengien, A. How does gpt-2 compute greater-than?: Interpreting mathematical abilities in a pre-trained language model. In *37th Conference on Neural Information Processing Systems*, 2023.
- Hyndman, R. J. and Khandakar, Y. Automatic time series forecasting: The forecast package for r. *Journal of Statistical Software*, 27(3):1–22, 2008.
- Hyndman, R. J., Athanasopoulos, G., Garza, A., Challu, C., Mergenthaler, M., and Olivares, K. G. *Forecasting: Principles and Practice, the Pythonic Way*. OTexts, Melbourne, Australia, 2024. available at <https://otexts.com/fpppy/>.
- Ismail Fawaz, H., Forestier, G., Weber, J., Idoumghar, L., and Muller, P.-A. Deep learning for time series classification: a review. *Data Mining and Knowledge Discovery*, 33(4):917–963, 2019.
- Jiang, J., Han, C., Jiang, W., Zhao, W. X., and Wang, J. Libcity: A unified library towards efficient and comprehensive urban spatial-temporal prediction, 2024. URL <https://arxiv.org/abs/2304.14343>.
- Lake, B. M. and Baroni, M. Generalization without systematicity: On the compositional skills of sequence-to-sequence recurrent networks. In *Proceedings of the 35th International Conference on Machine Learning*, 2018.
- Lim, B., Ö. Arık, S., Loeff, N., and Pfister, T. Temporal fusion transformers for interpretable multi-horizon time series forecasting. *International Journal of Forecasting*, 37(4):1748–1764, 2021.
- Liu, X., Liu, J., Woo, G., Aksu, T., Liang, Y., Zimmermann, R., Liu, C., Savarese, S., Xiong, C., and Sahoo, D. Moirai-moe: Empowering time series foundation models with sparse mixture of experts. *arXiv preprint arXiv:2410.10469*, 2024a.
- Liu, Y., Hu, T., Zhang, H., Wu, H., Wang, S., Ma, L., and Long, M. iTransformer: Inverted transformers are effective for time series forecasting, 2024b.
- Liu, Y., Qin, G., Huang, X., Wang, J., and Long, M. Timerxl: Long-context transformers for unified time series forecasting. *arXiv preprint arXiv:2410.04803*, 2024c.
- Liu, Y., Zhang, H., Li, C., Huang, X., Wang, J., and Long, M. Timer: Generative Pre-trained Transformers Are Large Time Series Models. In *Forty-first International Conference on Machine Learning*, 2024d.
- Mouatadid, S., Orenstein, P., Flaspohler, G., Oprescu, M., Cohen, J., Wang, F., Knight, S., Geogdzhayeva, M., Levang, S., Fraenkel, E., and Mackey, L. Subseasonalclimateusa: A dataset for subseasonal forecasting and benchmarking. In *37th Conference on Neural Information Processing Systems (NeurIPS 2023) Track on Datasets and Benchmarks*, 2023.
- Nair, V. and Hinton, J. E. Rectified linear units improve restricted boltzmann machines. In *ICML-23*, 2010.
- Ni, Z., Yu, H., Liu, S., Li, J., and Lin, W. Basisformer: Attention-based time series forecasting with learnable and interpretable basis. In *37th Conference on Neural Information Processing Systems*, 2024.
- Nie, Y., Nguyen, N. H., and an Jayant Kalagnanam2, P. S. A time series is worth 64 words: Long-term forecasting with transformers. In *Proceedings of the 11th International Conference on Learning Representations*, 2023.
- Olivares, K. G., Challu, C., Marcjasz, G., Weron, R., and Dubrawski, A. Neural basis expansion analysis with exogenous variables: Forecasting electricity prices with

- nbeatsx. *International Journal of Forecasting*, 39(2):884–900, 2022a.
- Olivares, K. G., Challú, C., Garza, F., Canseco, M. M., and Dubrawski, A. NeuralForecast: User friendly state-of-the-art neural forecasting models. PyCon Salt Lake City, Utah, US 2022, 2022b. URL <https://github.com/Nixtla/neuralforecast>.
- Oreshkin, B. N., Carпов, D., Chapados, N., and Bengio, Y. N-BEATS: neural basis expansion analysis for interpretable time series forecasting. In *8th International Conference on Learning Representations, ICLR 2020*, 2020. URL <https://openreview.net/forum?id=r1ecqn4YwB>.
- Rasul, K., Ashok, A., Williams, A. R., Ghonia, H., Bhagwatkar, R., Khorasani, A., Bayazi, M. J. D., Adamopoulos, G., Riachi, R., Hassen, N., Biloš, M., Garg, S., Schneider, A., Chapados, N., Drouin, A., Zantedeschi, V., Nevmyvaka, Y., and Rish, I. Lag-Llama: Towards foundation models for probabilistic time series forecasting, 2024.
- Rosenblatt, F. The perceptron: A probabilistic model for information storage and organization in the brain. *Psychological Review*, 65(6):386—408, 1958.
- Sak, H., Senior, A., and Beaufays, F. Long short-term memory based recurrent neural network architectures for large vocabulary speech recognition, 2014.
- Shi, X., Wang, S., Nie, Y., Li, D., Ye, Z., Wen, Q., and Jin, M. Time-moe: Billion-scale time series foundation models with mixture of experts. *arXiv preprint arXiv:2409.16040*, 2024.
- van den Oord, A., Dieleman, S., Zen, H., Simonyan, K., Vinyals, O., Graves, A., Kalchbrenner, N., Senior, A., and Kavukcuoglu, K. WaveNet: A generative model for raw audio, 2016.
- Vaswani, A., Shazeer, N., Parmar, N., Uszkoreit, J., Jones, L., and Gomez, A. N. Attention is all you need, 2017.
- Wang, B., Yue, X., Su, Y., and Sun, H. Grokked transformers are implicit reasoners: A mechanistic journey to the edge of generalization. In *38th Conference on Neural Information Processing Systems*, 2024.
- Wiliński, M., Goswami, M., Żukowska, N., Potosnak, W., and Dubrawski, A. Exploring representations and interventions in time series foundation models. *arXiv preprint arXiv:2409.12915*, 2024.
- Wolf, T., Debut, L., Sanh, V., Chaumond, J., Delangue, C., Moi, A., Cistac, P., Rault, T., Louf, R., Funtowicz, M., Davison, J., Shleifer, S., von Platen, P., Ma, C., Jernite, Y., Plu, J., Xu, C., Scao, T. L., Gugger, S., Drame, M., Lhoest, Q., and Rush, A. M. Transformers: State-of-the-art natural language processing. In *Proceedings of the 2020 Conference on Empirical Methods in Natural Language Processing: System Demonstrations*, pp. 38–45, Online, October 2020. Association for Computational Linguistics. URL <https://www.aclweb.org/anthology/2020.emnlp-demos.6>.
- Wolff, M., Olivares, K. G., Oreshkin, B., Ruan, S., Yang, S., Katoch, A., Ramasubramanian, S., Zhang, Y., Mahoney, M. W., Efimov, D., and Quenneville-Bélaire, V. ♠ SPADE ♠: Split peak attention decomposition. In *Thirty-Eighth Annual Conference on Neural Information Processing Systems NeurIPS 2024*, volume Time Series in the Age of Large Models Workshop, Vancouver, Canada, 2024. NeurIPS 2024. URL <https://arxiv.org/abs/2411.05852>.
- Woo, G., Liu, C., Kumar, A., Xiong, C., Savarese, S., and Sahoo, D. Unified training of universal time series forecasting transformers. In *Proceedings of the 41st International Conference on Machine Learning*, 2024.
- Wu, H., Xu, J., Wang, J., and Long, M. Autoformer: Decomposition transformers with auto-correlation for long-term series forecasting, 2021.
- Wu, H., Hu, T., Liu, Y., Zhou, H., Wang, J., and Long, M. TimesNet: Temporal 2d-variation modeling for general time series analysis. In *Proceedings of the 34th International Conference on Learning Representations*, 2023.
- Yang, R., Cao, L., Li, J., and Yang, J. Rethinking fourier transform from a basis functions perspective for long-term time series forecasting. 2024a.
- Yang, S., Gribovskaya, E., Kassner, N., Geva, M., and Riedel, S. Do large language models latently perform multi-hop reasoning? *arXiv preprint arXiv:2402.16837*, 2024b.
- Yao, Q., Yang, C.-H. H., Jiang, R., Liang, Y., Jin, M., and Pan, S. Towards neural scaling laws for time series foundation models. *arXiv preprint arXiv:2410.12360*, 2024.
- Zeng, A., Chen, M., Zhang, L., and Xu, Q. Are transformers effective for time series forecasting? In *Proceedings of the AAAI Conference on Artificial Intelligence*, 2023.
- Zhong, Z., Wu, Z., Manning, C. D., Potts, C., and Chen, D. MQuAKE: Assessing knowledge editing in language models via multi-hop questions. *arXiv preprint arXiv:2305.14795*, 2023.
- Zhou, H., Zhang, S., Peng, J., Zhang, S., Li, J., Xiong, H., and Zhang, W. Informer: Beyond efficient transformer for long sequence time-series forecasting, 2021.

Zhou, T., Fu, D., Sharan, V., and Jia, R. Pre-trained large language models use fourier features to compute addition, 2024.

Żukowska, N., Goswami, M., Wiliński, M., Potosnak, W., and Dubrawski, A. Towards long-context time series foundation models. *arXiv preprint arXiv:2409.13530*, 2024.

A. Supplemental Information

A.1. Extended Prior Work

Reasoning in LLMs. While models can recall individual facts well in single-hop Q&A tasks, they generally struggle with multi-hop reasoning that requires ‘chain-of-thought’ logic. Yang et al. (2024b) found evidence of latent multi-hop reasoning for specific fact compositions, but noted it is highly contextual. Wang et al. (2024) demonstrated that Transformers can learn implicit reasoning, but only after extended training beyond typical overfitting thresholds. Composition tasks have also been studied in machine translation, testing whether models can generalize learned command components to new conjunctions, such as repeating actions (Lake & Baroni, 2018).

Other types of reasoning studied in LLMs include *comparison* and *inverse search* (Allen-Zhu & Li, 2023; Wang et al., 2024). *Comparison* reasoning involves models evaluating two or more entities to make judgments to answer prompts of whether the attribute value of one entity is greater or smaller than that of another (Allen-Zhu & Li, 2023; Wang et al., 2024) or to complete numerical answers with appropriate ‘greater-than’ logic (Hanna et al., 2023). Inverse search tests a model’s ability to generate predictions in the reverse order of the training task. For example, this could involve applying the model to identify an entity based on its attributes when it was originally trained to predict the attributes of entities. Allen-Zhu et al. found that generative models struggle with inverse search unless trained specifically for it (Allen-Zhu & Li, 2023).

Time Series Reasoning with LLMs. Previous work has explored LLMs’ ability to understand and interpret time series concepts, such as slope and frequency, and translate them into meaningful natural language features. (Cai et al., 2024; Chow et al., 2024). This research differs from ours as it evaluates LLMs’ reasoning about or with time series concepts. In contrast, our work does not study LLMs but instead examines whether time series forecasting models can reason with time series.

Frequency-Based Modeling. While not focused on model reasoning, prior work in time series forecasting has used frequency-based features to improve performance. NBEATS reconstructs and forecasts time series by predicting Fourier coefficients needed for reconstruction, while BasisFormer similarly predicts these coefficients (Ni et al., 2024). Yang et al. leverage the Fourier basis expansion to provide frequency features directly in the time domain (Yang et al., 2024a). TimesNet utilizes the Fast Fourier Transform (FFT) to identify and extract significant frequency components indicative of periodic patterns (Wu et al., 2023). Previous models aim to improve architectures by incorporating frequency-based features during training. In contrast, our study focuses on evaluating whether models can logically generalize to unseen periodic patterns through the synthesis of frequency-based features—specifically, sine and cosine basis functions.

A.2. Models

DLinear (DLinear) - Linear layers are employed to model the trend and seasonal components, with the decomposition achieved through a moving average filter to separate the time series into its trend and seasonal components (Zeng et al., 2023).

NLinear (NLinear) - A Linear layer is employed to model the series. The model first subtracts the input by the last value of the sequence. Then, the input goes through a linear layer, and the subtracted part is added back before making the final prediction (Zeng et al., 2023).

Multi Layer Perceptron (MLP) - A neural network architecture composed of stacked Fully Connected Neural Networks trained with backpropagation (Nair & Hinton, 2010; Fukushima, 1975; Rosenblatt, 1958).

Neural Hierarchical Interpolation for Time Series (NHITS) - A deep learning model that applies multi-rate input pooling, hierarchical interpolation, and backcast residual connections together to generate additive predictions with different signal bands (Challu et al., 2022).

Neural Basis Expansion Analysis for Time Series (NBEATS) - A deep learning, MLP-based model that leverages both backward and forward residual connections. The network can decomposes the input signal into trend and seasonality components using polynomial and harmonic basis projections or substitute the polynomial and harmonic basis for identity basis based on the specified configuration (Oreshkin et al., 2020).

Time-Series Mixer (TSMixer) - TSMixer is a deep learning, MLP-based model that uses stacked mixing layers to learn and combine temporal and cross-sectional representations through mixing operations along both time and feature dimensions (Chen et al., 2023).

Long Short-Term Memory Recurrent Neural Network (LSTM) - A recurrent neural network (RNN) architecture that transforms hidden states from a multi-layer LSTM encoder into contexts which are used to generate forecasts using MLP s (Sak et al., 2014).

Temporal Convolution Network (TCN) - A 1D causal-convolutional network architecture that transforms hidden states into contexts which are used as inputs to MLP decoders to generate forecasts. Causal convolutions are used to generate contexts by convolving the prediction at time t only with elements from time t and earlier (Bai et al., 2018; van den Oord et al., 2016).

TimesNet (TimesNet) - A deep learning architecture that transforms the original 1D time series into a set of 2D tensors based on multiple periods to capture intra- and inter-period variations modeled by 2D kernels (Wu et al., 2023).

VanillaTransformer (VanillaTransformer) - An encoder-decoder architecture with a multi-head attention mechanism that uses autoregressive features from a convolution network, window-relative positional embeddings from harmonic functions, and absolute positional embeddings from calendar data. An MLP decoder outputs time series predictions in a single pass (Vaswani et al., 2017; Zhou et al., 2021).

iTransformer (iTransformer) - An attention-based deep learning architecture that applies attention and feed-forward networks to inverted dimensions by embedding time points into variate tokens. The attention mechanism capture multivariate correlations while the feed-forward network learns nonlinear representations for each token (Liu et al., 2024b).

Autoformer (Autoformer) - An encoder-decoder architecture with a multi-head attention mechanism that uses autoregressive features from a convolution network and absolute positional embeddings from calendar data. Decomposed trend and seasonal components are obtained using a moving average filter and an Auto-Correlation mechanism is used to identify periodic dependencies and aggregate similar sub-series (Wu et al., 2021; Vaswani et al., 2017).

Informer (Informer) - An encoder-decoder architecture with a multi-head attention mechanism that has three key features: a ProbSparse self-attention mechanism with $O(L \log L)$ complexity, a self-attention distilling process, and an MLP decoder that outputs time-series predictions in a single pass. It uses autoregressive features from a convolution network, window-relative positional embeddings from harmonic functions, and absolute positional embeddings from calendar data (Zhou et al., 2021; Vaswani et al., 2017).

Temporal Fusion Transformer (TFT) - An attention-based deep learning architecture that learns temporal relationships at different scales using LSTM s for local processing and self-attention layers to model long-term dependencies. It also leverages variable selection networks and a series of gating layers to suppress unnecessary processing in the architecture (Lim et al., 2021).

Patch Time Series Transformer (PatchTST) - An encoder-only, multi-head attention-based architecture that separates input time series into sub-series level patches as input tokens. Each channel is dedicated to a single univariate time series, and all channels use the same embedding and Transformer weights. (Nie et al., 2023)

T5-Efficient - A series of transformer-based architectures developed to enhance the efficiency of the original T5. Code and configuration files are open-source and obtained from the HuggingFace library (Wolf et al., 2020).

A.3. TSFM Model Design Decision Comparison

TSFMs involve combinations of various architectural component design decisions. We outline the design decisions of various TSFMs, including Chronos (Ansari et al., 2024a;b), LagLlama (Rasul et al., 2024), Moirai (Woo et al., 2024), MOMENT (Goswami et al., 2024b), Timer (Liu et al., 2024d), TimesFM (Das et al., 2024), and TinyTimeMixers (Ekambaram et al., 2024) in Table 2. These decisions encompass architectural choices, input series tokenization methods, projection layer types, and positional encodings, among others.

Table 2. Key design choices of widely used time series foundation models. All these models are based on the Transformer Architecture, with the exception of TinyTimeMixers (Ekambaram et al., 2024) which is an all-MLP architecture. All models which use Reversible Instance Normalization (RevIn), do so without the affine learnable parameters.

TSFM Component		Chronos	LagLlama	Moirai	MOMENT	Timer	TimesFM	TinyTimeMixers
Architecture	Encoder-Only	-	✓	✓	✓	-	-	-
	Decoder-Only	-	✓	-	-	✓	✓	-
	Encoder-Decoder	✓	-	-	-	-	-	✓
Tokenization	Fixed-Length Patches	-	-	-	✓	✓	✓	-
	Multi-Scale Patches	-	-	✓	-	-	-	-
	Adaptive-Length Patches	-	-	-	-	-	-	✓
	Binning	✓	-	-	-	-	-	-
	Lags	-	✓	-	-	-	-	-
Projection Layer	Linear	-	✓	✓	✓	✓	-	✓
	Residual	-	-	-	-	-	✓	-
Positional Encoding	Relative	-	-	-	✓	-	-	-
	SinCos	-	-	-	✓	✓	✓	(optional)
	RoPE	-	✓	✓	-	-	-	-
Loss	MAE	-	-	-	-	-	-	-
	MSE	-	-	-	✓	✓	✓	✓
	Huber	-	-	-	-	-	-	-
	Distribution	-	✓ (StudentT)	✓ (Mixture)	-	-	-	-
	Cross-Entropy	✓	-	-	-	-	-	-
Temporal Scaler	RevIN	-	-	✓	✓	✓	✓	✓
	Robust	-	✓	-	-	-	-	-
	Mean Absolute	✓	-	-	-	-	-	-

A.4. TSFM Design Decision Experiments

Comparing the performance of open-source TSFMs on compositional reasoning tasks alone does not allow us to isolate performance improvements attributable to specific components. To address this, we implement a deep learning Transformer architecture with a modular design, built on the open-source T5-efficient backbone (Wolf et al., 2020) to enable controlled experimentation with common TSFM design choices. An outline of the various types of components and methods for each design decision ablation is shown in Table 3.

Table 3. Hyper-parameters used in the TSFM experiments, with default hyper-parameters in **bold**.

Experiment	Experiment Parameters
Model Size :	T5-efficient- {tiny, mini, small, base}
Attention :	{Bidirectional, Casual}
Projection/Head Layer :	{Linear, Residual}
Tokenization :	{None, Fixed-patch length, Binning, Lags (l=2)}
Fixed-Patch Length :	{8, 16, 32, 64, 96, 128}
Positional Encoding :	{Relative, SinCos, Relative+SinCos, RoPE}
Loss Function :	{MAE, MSE, Huber, Distribution (StudentT, q=[80, 90])}
Scaler :	{RevIN (standard, non-learnable), Robust}
Context Length :	{256, 512}
Decomposition :	{None, Moving Avg.}

A.5. Synthetic Data

We leverage open-source code from MOMENT (Goswami et al., 2024b) to generate synthetic sinusoidal time series with varying frequency b and amplitude a : $\mathcal{F} = \{\mathcal{Y} : \mathcal{Y}(t) = a \sin(b2\pi t), a \cos(b2\pi t)\}$, where $a \in [1, 32]$ and $b \in [3, 32]$.

A.6. Real-World Data

Table 4 summarizes the characteristics of the real-world datasets used in our experiments. The ‘‘Pre’’ column denotes the dataset properties prior to preprocessing, while ‘‘Post’’ reflects the properties after preprocessing. For the real-world datasets, we selected a horizon length of 48, following the GIFT-Eval benchmark (Aksu et al., 2024). Please see section 3.2 for more details regarding data preprocessing.

Table 4. Dataset characteristics including domain, frequency, number (#) of series and number of forecast targets. The number of unique series in each dataset before (Pre) and after (Post) preprocessing are shown, as we selected 100 subseries to ensure consistent dataset sizes with an equal number of series and a training length of 1056 timesteps.

Dataset	Domain	Frequency	# Series (Pre)	# Series (Post)	# Targets	# Subseries (Post)	Series Length (Post)	Prediction Horizon
Synthetic Sinusoid	N/A	N/A	N/A	N/A	1	100	1,200	192
ECL	Energy	Hourly	321	47	1	100	1056	48
ETTm2	Energy	15 minute	1	1	7	100	1056	48
Solar	Energy	Hourly	5166	99	1	100	1056	48
Subseasonal	Climate	Weekly	862	56	4	100	1056	48
Loop Seattle	Transportation	Hourly	323	36	1	100	1056	48

A.7. Model Training and Parameters

All models are open-source. Models trained on synthetic data can be found in the `NeuralForecast` library (Olivares et al., 2022b). All models were trained and evaluated on a computing cluster consisting of 128 AMD EPYC 7502 CPUs, 503 GB of RAM, and 8 NVIDIA RTX A6000 GPUs each with 49 GiB RAM. The synthetic datasets used in our study will be released publicly with the full paper. The T5 backbone and configuration files are available in the Hugging Face library (Wolf et al., 2020).

We train the `T5 Model` with the following parameters outlined in Table 5 to ensure consistent evaluation across architectures. The training loss functions used in the ‘loss function’ ablation experiment include Mean absolute Error (MAE), Mean Squared Error (MSE), Huber Loss, and Distribution Loss with the Student’s t -distribution. H refers to the forecast horizon, t refers to the time point at which forecasts are generated, \mathbf{y} refers to the target signal values, and $\hat{\mathbf{y}}$ refers to the model’s predicted values:

$$\begin{aligned} \text{MAE}(\mathbf{y}_i, \hat{\mathbf{y}}_i) &= \frac{1}{H} \sum_{i=t+1}^{t+H} |\mathbf{y}_i - \hat{\mathbf{y}}_i|, & \text{Huber}(\mathbf{y}_i, \hat{\mathbf{y}}_i, \delta) &= \begin{cases} \frac{1}{2}(\mathbf{y}_i - \hat{\mathbf{y}}_i)^2, & \text{if } |\mathbf{y}_i - \hat{\mathbf{y}}_i| \leq \delta, \\ \delta \cdot (|\mathbf{y}_i - \hat{\mathbf{y}}_i| - \frac{1}{2}\delta), & \text{otherwise.} \end{cases}, \\ \text{MSE}(\mathbf{y}_i, \hat{\mathbf{y}}_i) &= \frac{1}{H} \sum_{i=t+1}^{t+H} (\mathbf{y}_i - \hat{\mathbf{y}}_i)^2, & \text{DistributionLoss}(\theta) &= -\log(P(\mathbf{y}_i|\theta)), \end{aligned}$$

where the probability density function (PDF) of the Student’s t -distribution with location parameter μ , scale parameter σ , and degrees of freedom ν is given by:

$$\mathbb{P}(\mathbf{y}_\tau | \mu, \sigma, \nu) = \frac{\Gamma(\frac{\nu+1}{2})}{\sqrt{\nu\pi} \Gamma(\frac{\nu}{2}) \sigma} \left(1 + \frac{1}{\nu} \left(\frac{\mathbf{y}_\tau - \mu}{\sigma} \right)^2 \right)^{-\frac{\nu+1}{2}},$$

Table 5. Common hyperparameter search space. † Based on the T5-efficient-tiny architecture

Hyperparameter	Considered Values
Input size :	256 (192 for tokenization experiments)
Learning rate :	1e-4
Batch size :	4
Windows batch size :	256
Dropout :	0.0
Training steps :	10000
Validation check steps :	100
Early stop patience steps :	20
Random seed :	{1, 5, 10}
Hidden size :	256†
Linear hidden size :	1024†
Model Encoder layers :	4†
Model Decoder layers :	0
Number of attention heads :	4†
Patch length :	96 for fixed-length patches (1 for other tokenization methods)
Stride :	8 for fixed-length patches (1 for other tokenization methods)

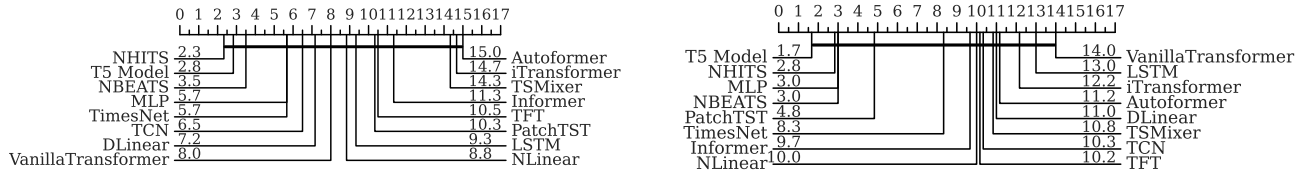
A.8. Evaluation Metrics

We use **Mean Absolute Error (MAE)** to evaluate model performance. Here, H refers to the forecast horizon, t refers to the time point at which forecasts are generated, \mathbf{y} refers to the target signal values, and $\hat{\mathbf{y}}$ refers to the model’s predicted values:

$$\text{MAE}(\mathbf{y}_\tau, \hat{\mathbf{y}}_\tau) = \frac{1}{H} \sum_{\tau=t+1}^{t+H} |\mathbf{y}_\tau - \hat{\mathbf{y}}_\tau|. \tag{10}$$

B. Supplemental Results

B.1. Model Rank and Pairwise Comparisons



(a) Model choice for in-distribution series (p-value: 2.71e-8)

(b) Model choice for out-of-distribution series (p-value: 3.52e-8)

Figure 7. Critical Difference (CD) diagrams illustrate model ranks and pairwise statistical comparisons of model performance on compositional reasoning tasks across all datasets. Lower ranks indicate better performance. A thick horizontal line groups models that are not significantly different. The statistical tests used to generate the CD diagrams are detailed in Section 3.4. (a, b) The patch-based Transformer models and MLP-based models outperform other models in both traditional and compositional reasoning forecasting paradigms. The Friedman p-value is included in the subtitles.

Implicit Reasoning in Deep Time Series Forecasting

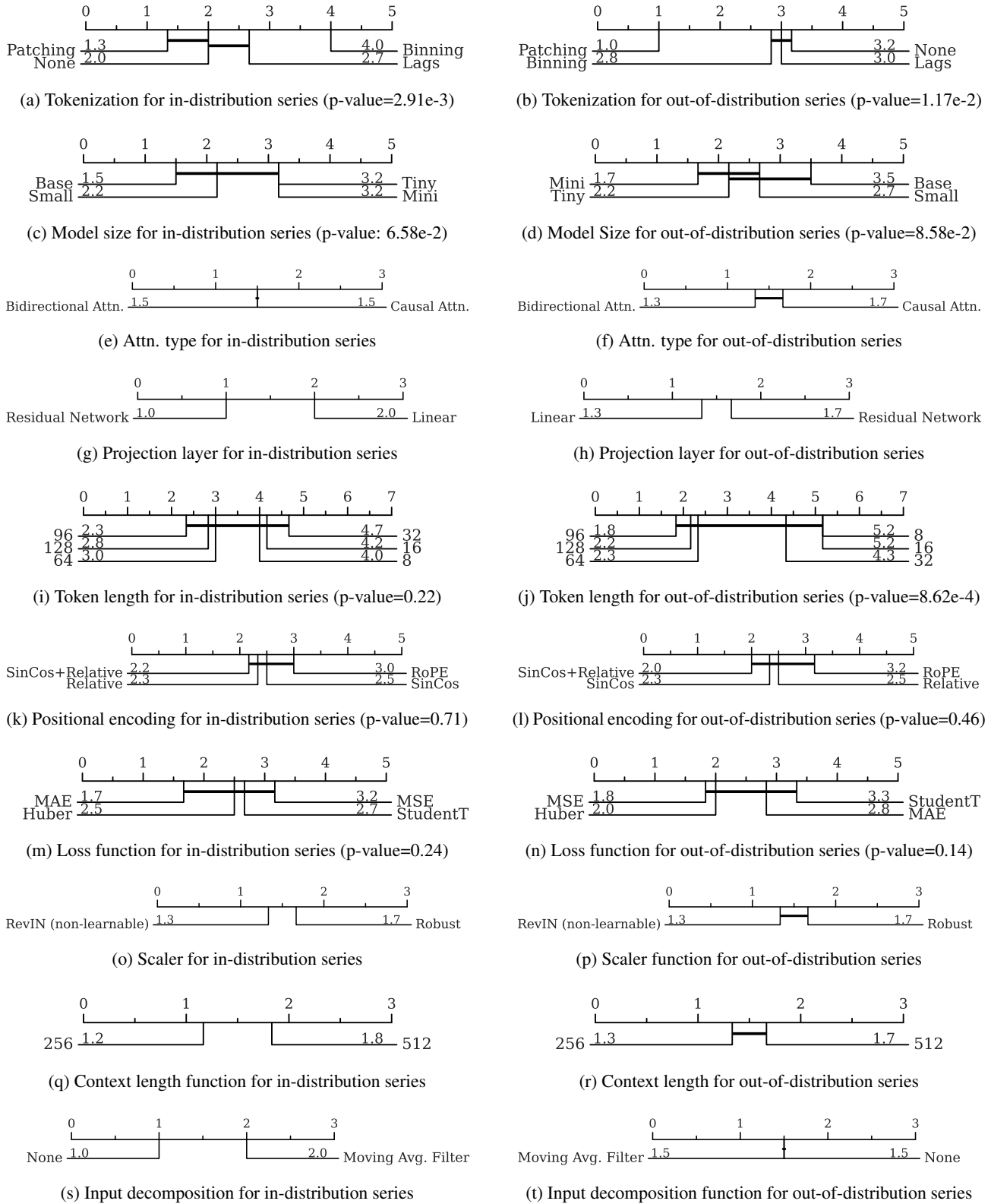
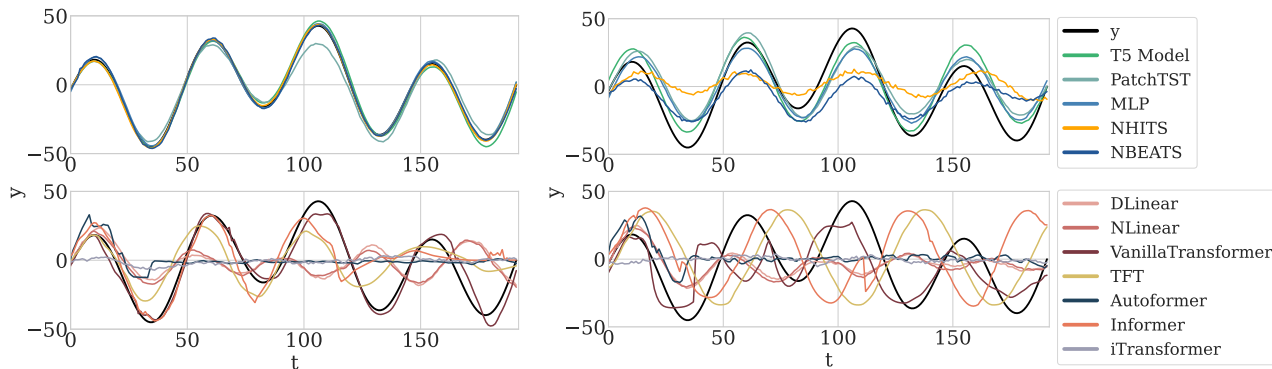


Figure 8. Critical Difference (CD) diagrams illustrate model ranks and pairwise statistical comparisons of model performance on compositional reasoning tasks across all datasets. Lower ranks indicate better performance. A thick horizontal line groups models that are not significantly different. The statistical tests used to generate the CD diagrams are detailed in Section 3.4. For analyses comparing three or more methods, the Friedman p-value is included in the subcaptions.

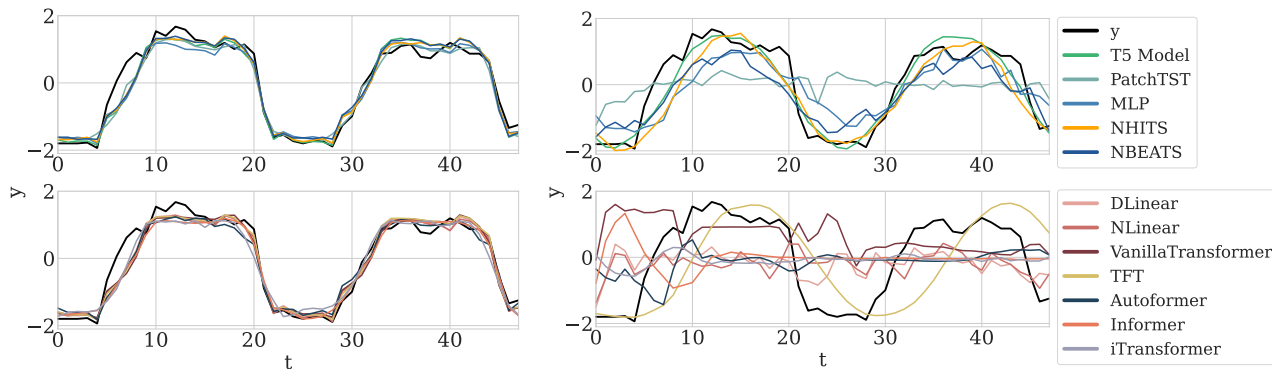
B.2. Model Forecasts

We include example forecasts for each of the 6 datasets used in this study.



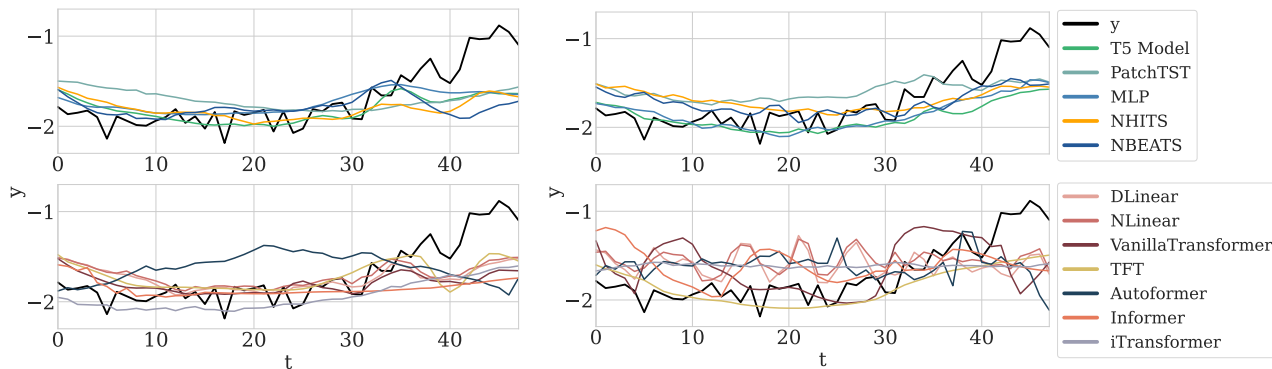
(a) Model forecasts for in-distribution Sinusoid series

(b) Model forecasts for out-of-distribution Sinusoid series



(c) Model forecasts for in-distribution ECL series

(d) Model forecasts for out-of-distribution ECL series



(e) Model forecasts for in-distribution ETTm2 series

(f) Model forecasts for out-of-distribution ETTm2 series

Figure 9. (a, c, e) Forecasts for a ground truth series $y(t)$ for the Sinusoid, ETTm2, and ECL datasets for models trained using the traditional forecasting paradigm. (b, d, f) Forecasts for the Sinusoid, ETTm2, and ECL datasets for models trained using the compositional reasoning forecasting paradigm. Patch-based Transformer models and MLP-based models (top), which rank among the top-performing models, demonstrate generalization to out-of-distribution time series, whereas other Transformer variants and linear models struggle to do so (bottom).

Implicit Reasoning in Deep Time Series Forecasting

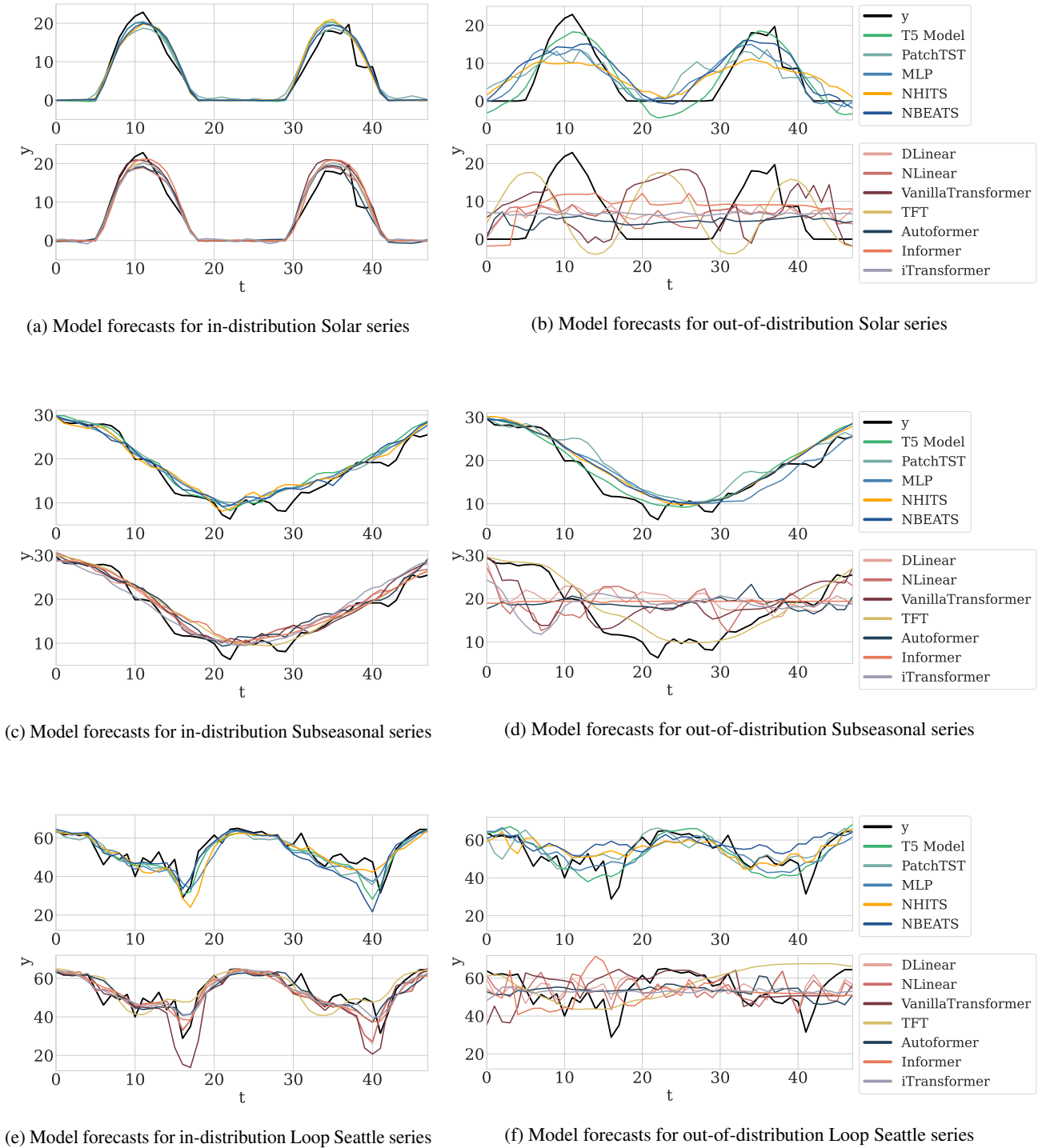


Figure 10. **(a, c, e)** Forecasts for a ground truth series $y(t)$ for the Solar, Subseasonal, and Loop Seattle datasets for models trained using the traditional forecasting paradigm. **(b, d, f)** Forecasts for a ground truth series $y(t)$ for the Solar, Subseasonal, and Loop Seattle datasets for models trained using the compositional reasoning forecasting paradigm. Patch-based Transformer models and MLP-based models (top), which rank among the top-performing models, demonstrate generalization to out-of-distribution time series, whereas other Transformer variants and linear models struggle to do so (bottom).

B.3. Model Performance, Efficiency, and Size Comparison

We rank model performance across datasets and compare rank with model computational complexity in terms of floating-point operations per second (FLOPs) and model size in terms of the total number of trainable parameters.

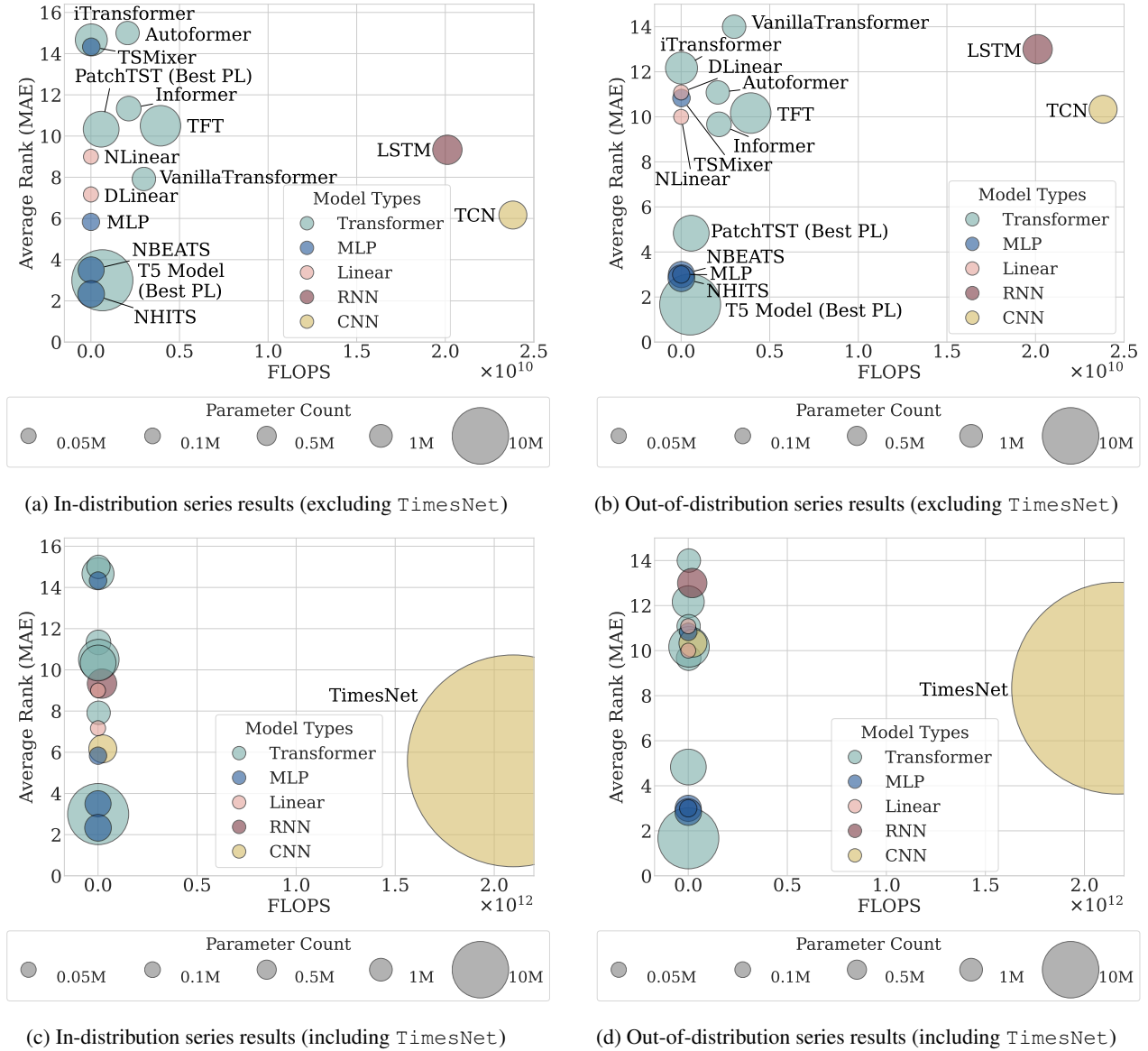


Figure 11. Comparison of average rank across datasets and random seeds versus model computational complexity, measured by floating-point operations per second (FLOPs). The size of each point represents the number of trainable parameters, highlighting the trade-offs between model complexity and performance. (a) In-distribution and (b) out-of-distribution results for all models, excluding TimesNet, are shown to provide a clearer comparison by mitigating the parameter size skew. (c) In-distribution and (d) out-of-distribution results for all models, including TimesNet.

B.4. Model Composition Reasoning Results

We include the complete table results with MAE error mean and standard deviation measured across three random seeds. The results of the compositional reasoning task for 16 widely adopted time series forecasting models are included in Table 6. Composition reasoning task results for controlled ablations of architecture components used in TSFMs are shown in Table 7.

Table 6. Mean Absolute Error (MAE) averaged over 3 random seeds (with standard deviation in parentheses) for composition reasoning tasks. The out-of-distribution (OOD) column presents MAE results for models trained via the compositional reasoning forecasting paradigm. The in-distribution (ID) column presents MAE results for models trained via the traditional forecasting paradigm. The T5 Model with the best patch length (PL) from Table 7 is included. Best results are highlighted in **bold**, second best results are underlined. The count of instances across datasets where the model ranks in the top three for performance is shown in the second to last column with non-zero entries in **blue**. The average number of top k compositions the model can outperform over the datasets is shown in the last column with nonzero entries in **purple**.

Model	Synthetic Sinusoid		ECL		ETTM2		Solar		Subseasonal		Loop Seattle		Top 3 Win Count		Top k Basis Wins		
	OOD	ID	OOD	ID	OOD	ID	OOD	ID	OOD	ID	OOD	ID	OOD	ID	OOD	ID	
Statistical	ARIMA	-	15.538	-	0.822	-	0.332	-	9.687	-	7.855	-	8.638	0	0	-	0.5
	AutoETS	-	16.075	-	0.105	-	0.211	-	1.730	-	2.067	-	5.575	-	0	-	0.8
Linear	DLinear	12.991	12.460	0.820	<u>0.103</u>	0.330	0.135	9.925	1.555	8.042	1.496	9.085	4.293	0	2	0.2	55.5
	NLinear	13.287	13.056	0.801	0.104	0.325	0.136	9.681	<u>1.569</u>	8.436	1.509	9.026	4.307	0	1	0.3	53.7
MLP-Based	MLP	<u>8.647</u>	2.475	<u>0.283</u>	0.106	0.253	0.114	<u>4.826</u>	1.559	1.886	1.456	7.839	3.864	3	1	10.2	61.2
	NHITS	8.924	1.106	0.295	0.101	0.214	0.100	5.682	1.592	1.858	<u>1.135</u>	<u>7.747</u>	3.448	4	4	11.0	64.3
	NBEATS	8.907	1.383	0.294	<u>0.103</u>	<u>0.216</u>	<u>0.102</u>	5.852	1.599	<u>1.840</u>	1.177	7.763	3.479	5	4	11.2	61.8
	TSMixer	14.466	15.090	0.799	0.129	0.335	0.182	9.877	1.979	7.770	1.602	8.865	5.565	0	0	0.3	19.7
RNN	LSTM	13.410	4.238	0.835	0.110	0.337	0.135	10.241	1.717	8.095	1.545	9.465	3.703	0	0	0	48.7
	TCN	11.478	3.833	0.837	0.106	0.339	0.135	9.868	1.642	6.170	1.234	8.792	<u>3.422</u>	0	1	0.7	55.7
CNN	TimesNet	9.788	<u>2.451</u>	0.518	0.104	0.313	0.109	9.914	1.714	4.109	1.500	9.872	2.970	0	2	2.3	52.8
	VanillaTransformer	12.279	4.935	0.919	0.106	0.334	0.136	11.956	1.667	9.641	1.276	11.675	3.591	0	0	0.2	54.8
Transformer	iTransformer	15.478	15.203	0.829	0.157	0.326	0.196	9.822	1.805	8.447	1.628	9.182	4.871	0	0	0.2	23.5
	Autoformer	15.301	15.018	0.795	0.137	0.330	0.294	10.348	2.108	7.933	2.390	8.634	4.758	0	0	0.3	15.8
	Informer	14.353	10.144	0.787	0.128	0.321	0.141	8.351	1.662	6.878	1.564	11.549	4.241	0	0	0.5	41.0
	TFT	14.531	9.745	0.445	0.115	0.312	0.117	12.873	2.106	2.684	1.454	11.280	5.340	0	0	4.7	28.5
	PatchTST (PL=8)	13.808	12.036	0.713	0.428	0.309	0.156	9.081	2.350	6.242	2.007	11.440	4.755	0	0	0.7	18.7
	PatchTST (PL=16)	14.133	13.633	0.666	0.279	0.253	0.150	10.788	1.633	5.877	1.904	9.855	4.989	0	0	0.8	27.8
	PatchTST (PL=32)	13.316	13.412	0.736	0.273	0.271	0.168	8.267	2.721	4.904	2.385	9.422	4.924	0	0	1.3	14.3
	PatchTST (PL=64)	12.232	13.544	0.482	0.122	0.247	0.169	8.054	2.813	2.292	1.754	10.529	4.405	1	0	6.8	27.2
	PatchTST (PL=96)	11.235	8.374	0.508	0.196	0.250	0.147	6.426	1.799	2.185	1.659	7.965	4.579	0	0	7.7	27.0
	PatchTST (PL=128)	10.696	6.959	0.832	0.161	0.323	0.138	5.726	1.964	2.448	1.678	9.378	3.653	0	0	5.7	32.7
T5 Model (Best PL)	7.177	2.480	0.239	<u>0.103</u>	0.259	0.103	3.899	1.578	1.714	1.097	6.589	3.351	5	4	12.2	64.3	

Implicit Reasoning in Deep Time Series Forecasting

Table 7. Mean Absolute Error (MAE) averaged over 3 random seeds (with standard deviation in parentheses) for composition reasoning tasks. The out-of-distribution (OOD) column presents MAE results for models trained via the compositional reasoning forecasting paradigm. The in-distribution (ID) column presents MAE results for models trained via the traditional forecasting paradigm. Best results are highlighted in **bold**. The count of instances across datasets where the model has the best performance is shown in the last column with non-zero entries in **blue**.

Transformer Model (T5 Backbone)		Synthetic Sinusoid		ECL		ETTm2		Solar		Subseasonal		Loop Seattle		Win Count	
		OOD	ID	OOD	ID	OOD	ID	OOD	ID	OOD	ID	OOD	ID	OOD	ID
Tokenization	None	14.032 (1.612)	4.894 (0.140)	0.685 (0.148)	0.106 (0.005)	0.369 (0.015)	0.121 (0.010)	9.969 (0.804)	1.635 (0.079)	6.401 (1.739)	1.572 (0.049)	14.327 (2.548)	3.766 (0.035)	0	2
	Fixed Length Patches	8.648 (0.072)	2.611 (0.158)	0.266 (0.019)	0.107 (0.002)	0.268 (0.003)	0.100 (0.003)	3.908 (0.204)	1.663 (0.023)	1.729 (0.028)	1.154 (0.029)	7.658 (0.100)	3.118 (0.026)	6	4
	Binning	17.039 (0.788)	9.504 (0.502)	0.833 (0.007)	0.270 (0.003)	0.317 (0.011)	0.199 (0.004)	8.445 (4.206)	4.719 (0.151)	3.758 (0.365)	3.253 (0.532)	12.728 (2.339)	7.735 (0.985)	0	0
	Lags	13.442 (0.254)	4.599 (0.328)	0.820 (0.178)	0.120 (0.005)	0.415 (0.046)	0.126 (0.006)	10.156 (1.364)	1.669 (0.030)	4.022 (0.187)	1.376 (0.043)	11.638 (1.556)	3.897 (0.074)	0	0
Model Size	Tiny	7.644 (0.025)	2.628 (0.108)	0.239 (0.005)	0.105 (0.002)	0.274 (0.005)	0.109 (0.006)	3.899 (0.578)	1.641 (0.068)	1.899 (0.203)	1.097 (0.039)	6.701 (0.153)	3.355 (0.053)	3	1
	Mini	7.882 (0.069)	2.318 (0.076)	0.242 (0.006)	0.107 (0.001)	0.273 (0.005)	0.103 (0.001)	3.810 (0.226)	1.663 (0.027)	1.769 (0.108)	1.104 (0.008)	6.888 (0.032)	3.018 (0.011)	3	0
	Small	8.057 (0.119)	2.103 (0.098)	0.268 (0.009)	0.103 (0.002)	0.268 (0.014)	0.096 (0.001)	4.172 (0.192)	1.665 (0.028)	1.770 (0.197)	1.048 (0.016)	6.924 (0.187)	2.764 (0.033)	0	0
	Base	8.308 (0.228)	2.084 (0.072)	0.247 (0.014)	0.100 (0.006)	0.274 (0.007)	0.091 (0.001)	4.338 (0.123)	1.667 (0.065)	1.853 (0.150)	0.967 (0.012)	7.005 (0.255)	2.536 (0.061)	0	5
Attn. Type	Bidirectional Attn.	7.644 (0.025)	2.628 (0.108)	0.239 (0.005)	0.105 (0.002)	0.274 (0.005)	0.109 (0.006)	3.899 (0.578)	1.641 (0.068)	1.899 (0.203)	1.097 (0.039)	6.701 (0.153)	3.355 (0.053)	4	3
	Causal Attn.	7.978 (0.02)	2.828 (0.233)	0.248 (0.005)	0.106 (0.004)	0.267 (0.010)	0.105 (0.003)	4.307 (0.144)	1.589 (0.042)	1.820 (0.173)	1.170 (0.054)	6.891 (0.133)	3.337 (0.044)	2	3
Proj./Head	Linear	7.644 (0.025)	2.628 (0.108)	0.239 (0.005)	0.105 (0.002)	0.274 (0.005)	0.109 (0.006)	3.899 (0.578)	1.641 (0.068)	1.899 (0.203)	1.097 (0.039)	6.701 (0.153)	3.355 (0.053)	4	0
	Residual	8.537 (0.184)	2.617 (0.043)	0.311 (0.011)	0.102 (0.002)	0.256 (0.008)	0.085 (0.003)	4.880 (0.389)	1.595 (0.039)	1.871 (0.296)	0.924 (0.016)	7.931 (0.655)	2.524 (0.028)	2	6
Token (Patch) Length	8	9.327 (0.28)	3.183 (0.117)	0.346 (0.040)	0.103 (0.001)	0.300 (0.013)	0.111 (0.003)	7.721 (0.640)	1.578 (0.009)	2.581 (0.335)	1.532 (0.002)	8.048 (0.108)	3.573 (0.047)	0	2
	16	9.007 (0.057)	3.573 (0.235)	0.418 (0.062)	0.105 (0.002)	0.283 (0.011)	0.103 (0.006)	9.139 (0.400)	1.673 (0.088)	2.731 (0.939)	1.362 (0.25)	8.499 (0.339)	3.510 (0.060)	0	1
	32	10.11 (0.07)	3.719 (0.190)	0.244 (0.011)	0.108 (0.004)	0.289 (0.007)	0.109 (0.002)	5.256 (0.591)	1.652 (0.071)	2.059 (0.171)	1.318 (0.187)	7.014 (0.167)	3.463 (0.015)	0	0
	64	8.747 (0.243)	2.971 (0.209)	0.239 (0.009)	0.106 (0.003)	0.285 (0.002)	0.107 (0.006)	4.201 (0.103)	1.651 (0.076)	1.819 (0.032)	1.265 (0.198)	6.589 (0.109)	3.408 (0.044)	2	0
	96	7.644 (0.025)	2.628 (0.108)	0.239 (0.005)	0.105 (0.002)	0.274 (0.005)	0.109 (0.006)	3.899 (0.578)	1.641 (0.068)	1.899 (0.203)	1.097 (0.039)	6.701 (0.153)	3.355 (0.053)	2	1
	128	7.177 (0.089)	2.480 (0.198)	0.255 (0.012)	0.107 (0.001)	0.259 (0.008)	0.107 (0.006)	4.385 (0.145)	1.673 (0.033)	1.714 (0.040)	1.100 (0.069)	6.878 (0.069)	3.351 (0.017)	3	2
Positional Encoding	Relative	7.751 (0.163)	2.750 (0.262)	0.284 (0.059)	0.105 (0.002)	0.268 (0.015)	0.111 (0.002)	4.373 (0.254)	1.640 (0.033)	1.826 (0.156)	1.093 (0.025)	6.883 (0.162)	3.337 (0.020)	2	2
	SinCos	7.881 (0.148)	2.456 (0.049)	0.247 (0.015)	0.104 (0.003)	0.270 (0.007)	0.112 (0.004)	4.357 (0.284)	1.624 (0.025)	1.839 (0.195)	1.464 (0.051)	6.818 (0.182)	3.366 (0.055)	0	3
	SinCos+Relative	7.644 (0.025)	2.628 (0.108)	0.239 (0.005)	0.105 (0.002)	0.274 (0.005)	0.109 (0.006)	3.899 (0.578)	1.641 (0.068)	1.899 (0.203)	1.097 (0.039)	6.701 (0.153)	3.355 (0.053)	4	1
	RoPE	7.921 (0.125)	2.701 (0.077)	0.255 (0.006)	0.104 (0.002)	0.274 (0.002)	0.112 (0.002)	4.608 (0.333)	1.647 (0.032)	1.872 (0.125)	1.106 (0.037)	6.721 (0.174)	3.378 (0.033)	0	1
Loss Function	MAE	7.644 (0.025)	2.628 (0.108)	0.239 (0.005)	0.105 (0.002)	0.274 (0.005)	0.109 (0.006)	3.899 (0.578)	1.641 (0.068)	1.899 (0.203)	1.097 (0.039)	6.701 (0.153)	3.355 (0.053)	1	3
	MSE	7.694 (0.178)	2.618 (0.088)	0.229 (0.006)	0.109 (0.004)	0.262 (0.007)	0.116 (0.010)	3.633 (0.466)	1.752 (0.030)	1.891 (0.193)	1.411 (0.214)	6.613 (0.118)	3.302 (0.045)	2	1
	Huber	7.648 (0.076)	2.914 (0.234)	0.234 (0.012)	0.108 (0.005)	0.264 (0.012)	0.112 (0.003)	4.035 (0.633)	1.746 (0.056)	1.801 (0.084)	1.258 (0.194)	6.571 (0.182)	3.281 (0.047)	2	1
	StudentT	7.776 (0.281)	2.660 (0.105)	0.244 (0.003)	0.104 (0.003)	0.270 (0.004)	0.113 (0.003)	4.134 (0.804)	1.648 (0.025)	1.735 (0.037)	1.377 (0.024)	6.872 (0.191)	3.543 (0.026)	1	1
Scaler	RevIN (Standard, non-learnable)	7.644 (0.025)	2.628 (0.108)	0.239 (0.005)	0.105 (0.002)	0.274 (0.005)	0.109 (0.006)	3.899 (0.578)	1.641 (0.068)	1.899 (0.203)	1.097 (0.039)	6.701 (0.153)	3.355 (0.053)	4	4
	Robust	7.931 (0.026)	2.725 (0.234)	0.326 (0.006)	0.103 (0.003)	0.270 (0.007)	0.106 (0.007)	8.170 (0.389)	1.734 (0.093)	1.736 (0.015)	1.232 (0.227)	6.982 (0.271)	3.412 (0.043)	2	2
Context	256	7.644 (0.025)	2.628 (0.108)	0.239 (0.005)	0.105 (0.002)	0.274 (0.005)	0.109 (0.006)	3.899 (0.578)	1.641 (0.068)	1.899 (0.203)	1.097 (0.039)	6.701 (0.153)	3.355 (0.053)	4	5
	512	7.072 (0.382)	2.605 (0.158)	0.253 (0.037)	0.111 (0.005)	0.298 (0.015)	0.151 (0.008)	4.187 (0.216)	1.740 (0.046)	1.934 (0.083)	1.829 (0.094)	6.295 (0.284)	4.013 (0.002)	2	1
Decomp.	None	7.644 (0.025)	2.628 (0.108)	0.239 (0.005)	0.105 (0.002)	0.274 (0.005)	0.109 (0.006)	3.899 (0.578)	1.641 (0.068)	1.899 (0.203)	1.097 (0.039)	6.701 (0.153)	3.355 (0.053)	4	6
	Moving Avg. Filter (DLinear, Autoformer)	6.726 (0.184)	2.860 (0.483)	0.265 (0.015)	0.106 (0.002)	0.264 (0.015)	0.112 (0.001)	4.018 (0.256)	1.663 (0.063)	1.769 (0.132)	1.252 (0.243)	6.942 (0.283)	3.470 (0.043)	2	0